Mathematical Biosciences and Engineering

http://www.aimspress.com/journal/mbe

MBE, 20(4): 6237–6272.
DOI: 10.3934/mbe.2023269
Received: 23 September 2022
Revised: 10 January 2023
Accepted: 11 January 2023
Published: 31 January 2023

Research article

Evaluating the impact of multiple factors on the control of COVID-19 epidemic: A modelling analysis using India as a case study

Aili Wang[1,2,*], Xueying Zhang[2], Rong Yan[2], Duo Bai[2] and Jingmin He[2]

[1] School of Science, Xi'an University of Technology, Xi'an 710054, China

[2] School of Mathematics and Information Science, Baoji University of Arts and Sciences, Baoji 721013, China

* **Correspondence:** Email: aily_wang83@163.com.

Abstract: The currently ongoing COVID-19 outbreak remains a global health concern. Understanding the transmission modes of COVID-19 can help develop more effective prevention and control strategies. In this study, we devise a two-strain nonlinear dynamical model with the purpose to shed light on the effect of multiple factors on the outbreak of the epidemic. Our targeted model incorporates the simultaneous transmission of the mutant strain and wild strain, environmental transmission and the implementation of vaccination, in the context of shortage of essential medical resources. By using the nonlinear least-square method, the model is validated based on the daily case data of the second COVID-19 wave in India, which has triggered a heavy load of confirmed cases. We present the formula for the effective reproduction number and give an estimate of it over the time. By conducting Latin Hyperbolic Sampling (LHS), evaluating the partial rank correlation coefficients (PRCCs) and other sensitivity analysis, we have found that increasing the transmission probability in contact with the mutant strain, the proportion of infecteds with mutant strain, the ratio of probability of the vaccinated individuals being infected, or the indirect transmission rate, all could aggravate the outbreak by raising the total number of deaths. We also found that increasing the recovery rate of those infecteds with mutant strain while decreasing their disease-induced death rate, or raising the vaccination rate, both could alleviate the outbreak by reducing the deaths. Our results demonstrate that reducing the prevalence of the mutant strain, improving the clearance of the virus in the environment, and strengthening the ability to treat infected individuals are critical to mitigate and control the spread of COVID-19, especially in the resource-constrained regions.

Keywords: nonlinear dynamical model; COVID-19; mutant strain; environmental transmission; effective reproduction number; sensitivity analysis

1. Introduction

The severe acute respiratory syndrome coronavirus 2 (SAR-CoV-2), which is responsible for COVID-19, is a type of highly contagious virus and has posed an unprecedent threat to public health worldwide. Since the first emerging in 2019, the virus has been spreading throughout the world and had a devastating impact not only on the high-income countries in Europe and North America but also in low and middle-income countries. As of 1 August 2022, there were 567,312,625 confirmed cases and 6,378,748 deaths of COVID-19 worldwide, making it the most far-reaching global health crisis since the 1918 influenza pandemic [1]. It has caused a ripple effect on the global economy including prolonged shutdowns and increased unemployment. Many a country or region has experienced multiple epidemic waves or outbreaks even with stringent interventions. So it is critical to explore the key reason for so many epidemic waves. In fact, there still exist quite a lot of urgent problems for those countries having experienced or experiencing multiple waves to solve including how to effectively prevent and control the spread of COVID-19 and how the impact of COVID-19 on public health and production can be reduced. So in this work, we will assess the efficiency of containments and provide insights with possible factors that aggravate the outbreak.

Since the outbreak of COVID-19, many dynamic models have been proposed to estimate the transmission risks, predict the final scale and evaluate the efficacy of non-pharmaceutical interventions on the control of the epidemic, which has important theoretical and practical significance [2–8]. Tang et al. [2] proposed a deterministic model and showed that intensive contact tracing can effectively reduce the potential and severity of the outbreak, especially in the early stage of the outbreak. Wu et al. [3, 4] assessed the effectiveness of major prevention and control strategies, including the quarantine and isolation, by building mathematical models and applying statistical methods. *Özköse* Fatma et al. [5] established a fractional epidemic model to test the relationship between the spread of COVID-19 and its correlation with diabetes. Huang et al. [6] constructed a mathematical model and used real-time data to determine peak time, peak size and final infection scale of the outbreak. Kumar et al. [7, 8] established mathematical models to explore the dynamics of COVID-19 epidemic in multiple susceptible populations and the transmission trend of COVID-19 in India. However, to the authors' best knowledge, few modelling studies have examined the role of multiple factors, such as shortage of medical resources, mutant strain, et al., on the spread of COVID-19.

India, as one of the countries facing shortage of medical resources, has experienced its second wave of COVID-19 pandemic from early March, 2021 and the daily number of confirmed cases was still more than 20,000 at the end of September, 2021, which has caused more than four million reported confirmed cases and four thousand reported deaths during the peak infection [9]. So in this work, we will take India as an example to reveal the key factors affecting the outbreak and development of the epidemic. In fact, the driving factors of virus transmission in India are various, including economics, seasonality, geo-environmental and climatic factor [10–12]. And the commercial trade is also an important factor which can accelerate the diffusion of COVID-19 [13]. In addition, India's high population density, sever shortage of medical resources, simultaneous spread of the wild and mutant strains have caused the epidemic to be so serious. In this work, we consider the medical resource-constraints, mutant strain, environmental transmission and assess the efficiency of these factors on the containment of the outbreak. Given that about 70% of the population was already vaccinated during this outbreak of COVID-19 in India, the effect of vaccine in controlling the outbreak was also taken

into account in the modelling, despite of low vaccine coverage.

India, as a populated dense country, has been struck by the second wave of COVID-19 severely with a overburdened healthcare system and significant case fatality rate, which has raised public health pressing concerns in the fight against the COVID-19 pandemic [14–16]. The high patient-to-doctor proportion 1456:1 besides the major imbalance in the size of healthcare workers and the size of people has added the difficulty in dealing with the second COVID-19 wave in India [17]. There are only about 8 physicians and 8.5 hospital beds for every 10,000 individuals. That, together with the overwhelming number of cases, are the maim burden borne by the healthcare workers. This phenomenon is even worse in rural India, where only 3.2 hospital beds are available for 10,000 individuals [18]. And for the states Uttar Pradesh, Rajasthan and Jharhand, there are only 2.5, 2.4 and 2.3 hospital beds every 10,000 individuals, respectively [19]. Medical-resource constraints is true in some of the developed countries [20]. Brendon et al. [21] has investigated the capacities of hospital beds, intensive care units (ICU) and acute care beds in more than 180 countries including the high-income countries, such as the United States and United Kingdom, and the middle countries, such as India. They found that the high-income countries have 12.79 ICU beds and 402.32 hospital beds every 10,000 individuals, but the rapid surge of cases has overwhelmed the available resources some time. The present studies highlight the viral role of medical resources in the outbreak of COVID-19. And there are research work that assessed the effect of medical resource in the spread of COVID-19 by developing mathematical models [20,22–24]. Zhu et al. [22,23] designed compartment models with three or two phases to explore the vital role of the hospital bed capacity in containing the outbreak of COVID-19 in Wuhan. They found that increasing hospital-bed capacity to isolate those infecteds with mild symptoms could help curb the outbreaks in regions with medical-resource constrained. Tang et al. [20, 24] proposed piecewise-defined models to reveal the effect of hospital bed shortages in the transmission of COVID-19 in certain regions. They highlighted the critical role of timely improvement of abilities to supplement medical resources in effective controlling the COVID-19 epidemic. However, how the shortage of hospital bed, together with other containments, affected the spread of COVID-19 in India has not yet been well evaluated.

Lin et al. [25] emphasizes the effect of various feature factors on the spread of COVID-19 epidemic. In fact, many a factor is involved in driving the second COVID-19 wave in India, such as the complex interplay of mutant strains with higher pathogenicity and environmental transmission caused by infected individuals' respiratory droplets, in the context of the medical-resource constraints. During the second COVID-19 wave in India, Delta strain, a type of new strain of COVID-19 characterized by rapid transmission and strong infectivity, is circulating in India [26, 27]. Because of the abundant genetic diversity and high evolution capability, SAR-CoV-2 has already exhibits dynamically evolving mutation [28–31]. Many a mutant strain of COVID-19 with high transmission rate was identified around the world, including the Beta strain in South Africa, Alpha strain in the UK and the Omicron strain in Gauteng province, South Africa [32]. Delta strain compromises the effectiveness of existing COVID-19 vaccines and leads to the insurgence of anti-microbial drug resistance, in addition to inducing a surge of cases and deaths in India [33, 34]. In fact, as the supply of COVID-19 vaccines increases, a mass vaccination campaign was implemented in India on January 16, 2021 with the first dose for 30 million front-line workers, including health care workers and security forces, and the second dose for those aged over 50 or under 50 but with multiple diseases. However, the efficiency of vaccines is reduced since Delta strain, as a mutant strain, can help the virus replicate more efficiently or escape the immune system [33]. More than one work has studied the effect of mutant strain and vac-

cination strategy on the transmission of the COVID-19 epidemic by formulating mathematical models [27, 30, 31, 34, 35]. Sonabend et al. [27, 30] proposed novel COVID-19 models to investigate how the vaccination and delta variant affect the outbreak of COVID-19 in England and Jiangsu China. They found that the increasing population immunity and lifting non-pharmaceutical interventions resulted in a decreasing of the transmission; while delta variant lead to an increasing of the peak size. Betti et al. [31] devised a two-strain mathematical model and used the data of COVID-19 epidemic in Ontario to parameterize the model. They found that a variant strain was unlikely to dominate in short period. Khyar et al. [34] investigated the global dynamics of a two-strain epidemic model, which can fit the COVID-19 clinical data well. Britto et al. [35] expanded and SEIR model to assess age-specific vaccine allocation strategies in India. The results supported global recommendations to prioritize COVID-19 vaccine allocation for older age groups. However, how much the vaccines help contain the outbreak by protecting the exposed individuals with Delta strain being infected, in the context of medical resource shortage, such as in countries like India, is not fully understood.

According to the updated scientific brief on COVID-19 transmission by WHO, the transmission modes of SARS-CoV-2 include contaminated environment besides close contact [36]. During the outbreak of second wave of COVID-19 in India, the virus, which was spread by respiratory droplets produced when infected individuals cough, sneeze, talk, et al., persists in the environment and on hard surfaces. There is study suggests that the virus can stay on plastic and stainless metal surfaces, such as door handles, desktops and tables, from two to three days [37]. Moreover, the transmission from improperly or not timely handled deceased cases to susceptibles is also a considerable way of transmission [38]. With the sudden rise in the number of deceased cases as well as shortage of medical resources in India, the deceased cases cannot be handled properly or in time [39], which releases virus into the environments. More than one research has revealed the indispensable role of contaminated environments in the outbreak of COVID-19 [40–43], which provides more information on the infected risk and infectivity of contaminated surfaces. Zu et al. [40] proposed a nonlinear mathematical model to analyze the effects of the environmental virus on the transmission patters. By fitting the targeted model to the data in India, they highlighted the necessity of reducing the virus in the environment. He et al. [41] proposed a novel dynamic model to assess the effect of environmental contribution in the transmission dynamics of COVID-19. By validating the model using the COVID-19 reported data in Saudi Arabia, they revealed the crucial role of environmental transmission in the outbreak. Wang et al. [42] formulated a mathematical model incorporating multiple transmission pathways and fitted the model to the publicly reported data in China. The result emphasized the important role of environmental reservoirs in the transmission of COVID-19. Babington-Ashaye et al. [43] did a scoping review to understand the risks of infection with COVID-19 via contaminated surfaces. They have selected 565 relevant articles and found that the risk of SARS-CoV-2 infection via contaminated surfaces assessed as low in the majority of the reviewed articles. As a result, the knowledge regarding the environmental transmission and transmission mechanism of COVID-19, especially in the case of the spread of mutant strain and shortage of medical resources, remains limited.

As a result, the second wave of COVID-19 pandemic in India has resulted in mass destruction due to the shortage of medical resource, heavy load of patients, spread of delta strain and environmental transmission although a vaccination strategy has been implemented. This outbreak have raised the pressing concerns of much of the world in the fight against the current pandemic. So it is necessary to provide insights into the lessons learnt from the second wave as well as the possible strategies could be

implemented to contain the viral spread. Up to this point, many mathematical models have focused on the spread and control strategies of COVID-19 from different perspectives [5, 20, 22–24, 27, 30, 31, 34, 35, 40–45]. These models were established based on the monitoring data of COVID-19 to capture the characteristics of the SAR-CoV-2, assess the risk of reinfection, evaluate the epidemic scale, explore the reasonable allocation of medical emergency resources, et al. However, the previous models only studied the impact of one or two factors on the tackling of the COVID-19 outbreak although. As known to all, many factors including the medical resource shortages, spread of mutant strain, environmental transmission and vaccination are reported to affect the second wave of COVID-19 outbreak in India. To the best of our knowledge, little work was done to mimic the the combined effect of multiple factors in the transmission and control of this outbreak. And it falls within the scope of this work.

To give a detailed understanding on how the simultaneous spread of the more pathogenic mutant strain and the wild strain, implementation of vaccination and indirect transmission caused by contaminated environments, in the context of shortage of medical resources, affect the outbreak of COVID-19 in the regions or countries with heavy population, it is urgent to quantitatively analyze the relationship between various factors and the outbreak of COVID-19. And the above introduction demonstrates that these problems are very prominent in India, especially the shortage of medical resources, so we chose India as an example to study. In this work, we propose a nonsmooth dynamic model for the COVID-19 pandemic incorporating the combined effects of these factors on the overall dynamics of the disease.

2. Materials and methods

• *Sample and data*

We obtained the data of COVID-19 cases in India from 1 March to 1 October 2021 from Baidu's Real Time Big Data Report on COVID-19 [9]. The data included the daily number of confirmed cases, recovered cases and deaths, as shown in Figure 1. Since the beginning of March, the daily number of confirmed cases has continuously climbed, which was the second major outbreak in India caused by the emergence of mutant strain and local large-scale gatherings. As of 1 October 2021, the cumulative number of confirmed cases, recovered cases and deaths climbed up to 33,789,398, 33,060,980 and 448,605, respectively. On 15 April when the huge religious gatherings held, the daily number of confirmed cases exceeded 200,000 for the first time and it took just a week to reach 315,800. On April 30, the number rose to more than 400,000, as shown in Figure 1(a).

As the outbreak in India got worse, many countries sent medical supplies to India, and then the daily number of recovered cases reached 422,394 on 17 May, which was the highest number of daily recovered cases, as shown in Figure 1(b). With the number of confirmed cases continuously rising and medical resources becoming inadequate severely, the daily number of reported deaths exceeded 1000 on 13 April and soon the daily number of reported deaths rose to 6,148 that was the highest number of new deaths in a single day in India, as shown in Figure 1(c). One of the reasons for such a big number of daily reported deaths was one of India's poorest state Bihar fixed the method of counting new deaths, following which 3951 deaths were added. However, those who died of post-COVID complications after testing negative were not included in the death toll. In this work, we assumed that only the deaths died in hospitals were included in the death toll.

In India, a mass vaccination campaign began on 16 January. The first phase was for 30 million front-line workers, such as health care workers and security forces. The second phase was for people

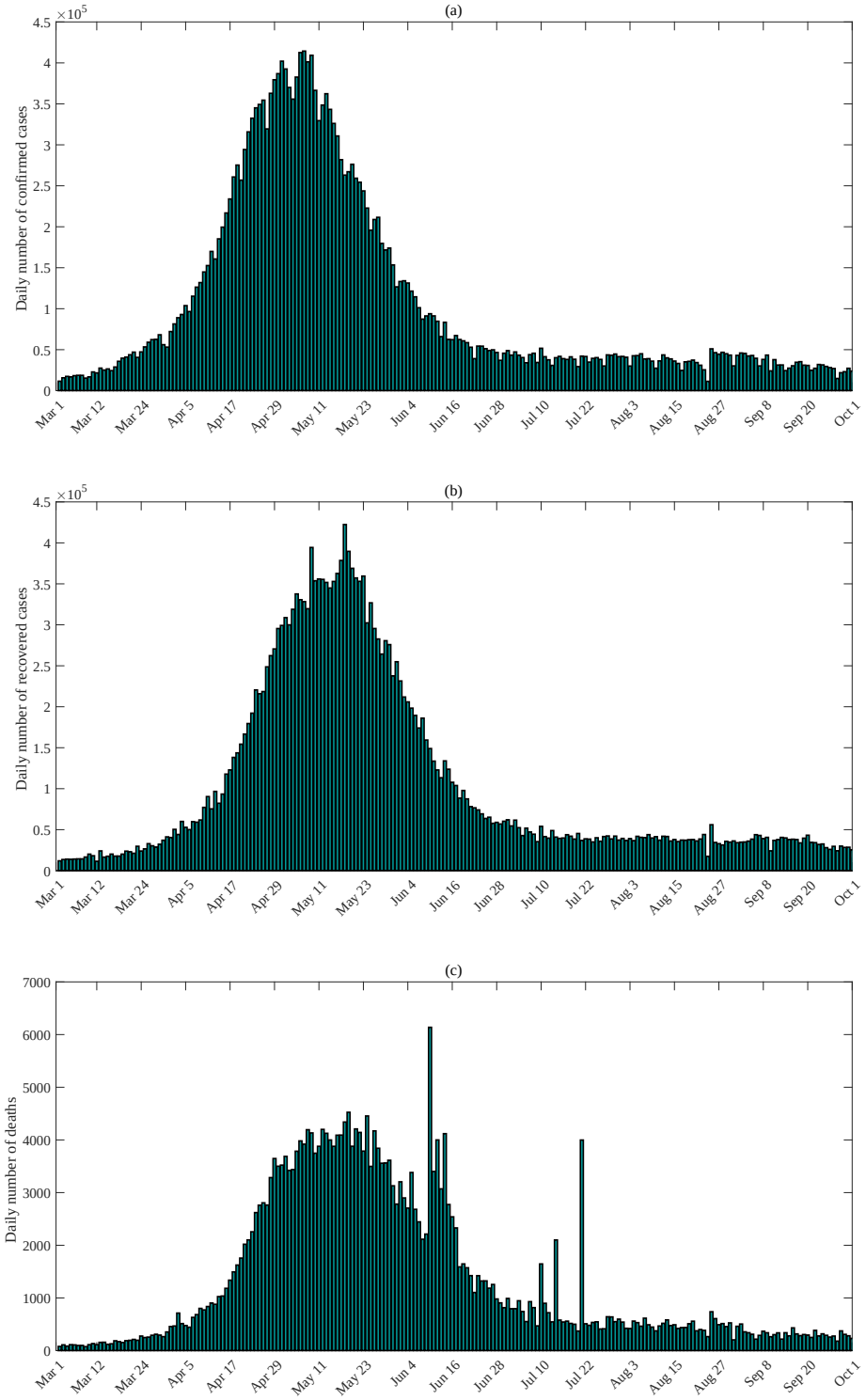

Figure 1. The data on COVID-19 in India from 1 March to 1 October 2021. (a) Daily reported confirmed cases; (b) Daily reported recovered cases; (c) Daily reported deaths.

aged over 50 and those under 50 with multiple diseases. Vaccination was available in more than 8,600 public and private hospitals since 1 March and vaccines are free for the public [7]. About 1 billion doses of vaccines has been completed in India. About 75 percent of the adults in India received at least one dose of the coronavirus vaccine, and about 30 percent of them have been fully vaccinated. So we consider the impact of vaccination on the spread of COVID-19 in India in this paper.

Shortage of hospital beds, oxygen, vaccines and medicines occurred in many parts of India as the outbreak aggravated dramatically. In some hospitals, there were 50 patients fighting for a bed. In Maharashtra, one of the states with severe outbreak, patients had to take shelter in ambulances, private cars and even electric three-wheelers with long queues at hospitals and patients lying in car parks taking oxygen [46, 47]. Thus we considered the impact of the shortage of essential medical resources on the spread in India. We used the capacity of hospital beds to evaluate the amount of medical resources in this work. Because of a lack of data on the number of hospital beds, and India government has been gradually strengthening their medical resources and other control measures, in particular, more and more beds were provided in response to the outbreak, we adopted a logistic model to estimate the number of hospital beds used to treat patients infected with COVID-19 in India. In fact, the logistic model has been successfully adopted to mimic the number of hospital beds in combating the outbreak of COVID-19 in China, South Korea, Japan, Italy, Spain and Iran [20].

• *Measures of variables*

In this work, we assumed that the number of hospital beds $H_c(t)$ was a constant H_{c0} before 1 March, and it was an increasing function submitted to the following logistic model

$$\frac{\mathrm{d}H_c(t)}{\mathrm{d}t} = rH_c(t)\left(1 - \frac{H_c(t)}{M}\right) \tag{2.1}$$

from then on. It is worth emphasizing that during the second wave of the COVID-19 outbreak in India, many a people shared a bed, so here $H_c(t)$ represented the number of people having hospital beds, not the number of hospital beds, and for simplicity, we will call $H_c(t)$ the number of hospital beds in the rest of this paper. In model (2.1), r denoted the net increasing rate of hospital beds and M stood for the maximum number of hospital beds in India during the COVID-19 outbreak. We embed model (2.1) into our targeted model and fitted the final model to the data on the daily number of confirmed cases, recovered cases and deaths to estimate the parameters, including r and M. Taking into account of the pivotal role of the indirect transmission caused by the contaminated environments in COVID-19 infection as introduced in Section 1, we also mimic the effects of contaminated environments on transmission dynamics in India in this work.

Denote T_0 as the date 9 April, 2021 when the lockdown strategy began to implement, T_1 as the date 31 May, 2021 when the containment measures were gradually lifted, T_2 as the date 27 April, 2021 when the first batch of medical aid from the UK arrived at the airport in Indian capital New Delhi, T_3 as the date 10 May, 2021 when the last batch of medical aid from China arrived in India, and T_4 as the date 10 July, 2021, since then the daily number of confirmed cases has been basically below 40,000 and the epidemic has been in effective control. Thus we assume the public awareness as well as the prevention and control measures were improved and strengthened gradually after 9 April, so we assumed that the contact rate $c(t)$, the diagnosis rates $\delta(t)$, the recovery rate $\gamma_H(t)$ and the disease-induced death rate $\alpha_H(t)$ of hospitalized individuals are time-dependent.

The contact rate $c(t)$ is assumed to be a constant before 9 April and a decreasing function with respect to time t after 9 April due to the implementation of lockdown strategies and the raising of public awareness. After 31 May, containment measures were gradually enhanced, and the contact rate became anther constant. So, $c(t)$ took the following form:

$$c(t) = \begin{cases} c_0, & t \le T_0, \\ (c_0 - c_1)e^{-r_c(t-T_0)} + c_1, & T_0 < t \le T_1, \\ c_1, & t > T_1, \end{cases} \tag{2.2}$$

where c_0 was the contact rate without control measures or awareness of the disease, $c_1(c_1 < c_0)$ was the minimum contact rate with the unprecedented intervention measures and self-isolation, r_c was the corresponding decreasing rate of the contact rate. Here $T_0 = 39, T_1 = 92$, since the data we used for model fitting started at 1 March 2021.

The period from onset of symptoms to being diagnosed ($\frac{1}{\delta}$) was gradually shortened due to the increasing of public awareness and medical assistance from multiple countries. The first batch of medical supplies from Britain arrived in India on 27 April, so the diagnosis rate $\delta(t)$ was an increasing function with respect to time t from 27 April to 10 May when the last batch of medical supplies from China arrived in India. From May 10 to July 10, the diagnosis rate $\delta(t)$ was assumed to be a decreasing function with respect to time t as the medical resources running out. After 10 July, the daily number of confirmed individuals has changed relatively little, so the diagnosis rate $\delta(t)$ was assumed to be a constant. Thus, the diagnosis period was described by the following piecewise-defined function:

$$\delta(t) = \begin{cases} \delta_0, & t \le T_2, \\ (\delta_0 - \delta_1)e^{-r_\delta(t-T_2)} + \delta_1, & T_2 < t \le T_3, \\ (\delta_1 - \delta_2)e^{-r_\delta(t-T_3)} + \delta_2, & T_3 < t \le T_4, \\ \delta_2, & t > T_4, \end{cases} \tag{2.3}$$

where $T_2 = 57, T_3 = 71, T_4 = 132, \delta_0$ was the initial diagnosis rate of infected individuals, $\delta_1(\delta_0 < \delta_1)$ was the maximum diagnosis rate of individuals, $\delta_2(\delta_0 < \delta_2 < \delta_1)$ was the final diagnosis rate of infected individuals and r_δ was the corresponding decreasing rate.

With the aid of medical resources from various countries, the recovery rate $\gamma_H(t)$ increased and the disease-induced death rate $\alpha_H(t)$ decreased before the end of medical assistance on 19 May. As the medical resources running out, the recovery rate $\gamma_H(t)$ was decreasing with respect to time t from 19 May to 10 July and it remained a constant after 10 July. As for the disease-induced death rate $\alpha_H(t)$, as the daily number of confirmed cases decreasing gradually and Indian government increasing the capacity of hospital beds, a large number of cases entered the hospital for treatment, so $\alpha_H(t)$ remained decreasing, but at a smaller decreasing rate from 19 May to 10 July; while it took a constant after 10 July. Thus $\gamma_H(t)$ and $\alpha_H(t)$ took the following form:

$$\gamma_H(t) = \begin{cases} \gamma_{H0}, & t \le T_2, \\ (\gamma_{H0} - \gamma_{H1})e^{-r_H(t-T_2)} + \gamma_{H1}, & T_2 < t \le T_3, \\ (\gamma_{H1} - \gamma_{H2})e^{-r_H(t-T_3)} + \gamma_{H2}, & T_3 < t \le T_4, \\ \gamma_{H2}, & t > T_4, \end{cases} \tag{2.4}$$

$$\alpha_H(t) = \begin{cases} \alpha_{H0}, & t \le T_2, \\ (\alpha_{H0} - \alpha_{H1})e^{-r_\alpha(t-T_2)} + \alpha_{H1}, & T_2 < t \le T_3, \\ (\alpha_{H1} - \alpha_{H2})e^{-r_\alpha(t-T_3)} + \alpha_{H2}, & T_3 < t \le T_4, \\ \alpha_{H2}, & t > T_4, \end{cases} \tag{2.5}$$

where γ_{H0} (resp. α_{H0}) was the recovery rate (resp. disease-induced death rate) of hospitalized individuals before 27 April, $\gamma_{H1}(\gamma_{H0} < \gamma_{H1})$ (resp. $\alpha_{H1}(\alpha_{H1} < \alpha_{H0})$ was the maximum recovery rate (resp. small disease-induced death rate), $\gamma_{H2}(\gamma_{H2} < \gamma_{H0} < \gamma_{H1})$ was the final recovery rate after two months of consuming of the medical resources from the foreign countries, $\alpha_{H2}(\alpha_{H2} < \alpha_{H1} < \alpha_{H0})$ was the minimum disease-induced death rate, r_H (resp. r_α) was the corresponding exponential changing rate of the recovery rate (resp. disease-induced death rate).

• *Models and data analysis procedure*

Based on the disease progression and the intervention measures, we extended the basic SEIR model by considering the wild and mutant strains of SARS-CoV-2 in India, contamination of the environment, vaccination, and constraints of medical resources on the spread of the epidemic. The population is divided into ten compartments: susceptible (S), vaccinated (V), exposed (E), undiagnosed infecteds with the wild strain (I_w), undiagnosed infecteds with the mutant strain (I_m), confirmed with the wild strain but not hospitalized (P_w), confirmed with the mutant strain but not hospitalized (P_m), confirmed and hospitalized (H), recovered (R) and deceased (D). The density of pathogen in the contaminated environments is denoted by W, as shown in Figure 2.

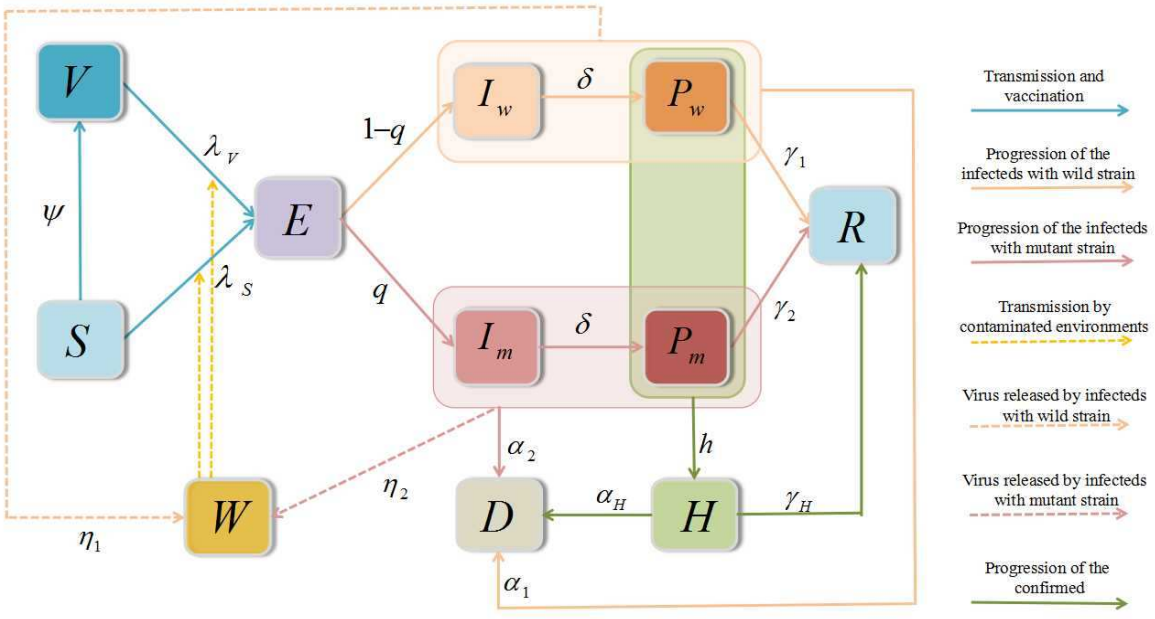

Figure 2. A schematic flow diagram of the transmission of COVID-19 with the simultaneous spread of the mutant strain and the wild strain.

The modelling framework SEIPR is used to describe the transmission dynamics, where the undiagnosed infecteds are divided into two classes according to the strain of infection: undiagnosed infecteds

with the wild strain (i.e., I_w) and with the mutant strain (i.e., I_m). For simplicity, we call I_m (resp. I_w) the infecteds with wild strain (resp. the infecteds with mutant strain) in the rest of this work. Due to the limitation of medical resources, some of the confirmed individuals enter the hospitalized class H with a certain admission rate, and the other confirmed individuals progress into the class R without receiving treatment. The virus in the environment can accelerate the infection of susceptibles and vaccinated individuals, as shown in Figure 2. The total population size is denoted by N, where $N = S + V + E + I_w + I_m + P_w + P_m + H + R$. The model is described by the following system of ordinary differential equations

$$\begin{cases} \frac{dS}{dt} = \lambda_S S - \Psi S, \\ \frac{dE}{dt} = \lambda_S S + \lambda_v V - \sigma E, \\ \frac{dI_w}{dt} = (1-q)\sigma E - \delta(t) I_w - \alpha_1 I_w, \\ \frac{dI_m}{dt} = q\sigma E - \delta(t) I_m - \alpha_2 I_m, \\ \frac{dP_w}{dt} = \delta(t) I_w - h(t) P_w - \gamma_1 P_w - \alpha_1 P_w, \\ \frac{dP_m}{dt} = \delta(t) I_m - h(t) P_m - \gamma_2 P_m - \alpha_2 P_m, \\ \frac{dH}{dt} = h(t)(P_w + P_m) - \gamma_H(t) H - \alpha_H H, \\ \frac{dR}{dt} = \gamma_H(t) H + \gamma_1 P_w + \gamma_2 P_m, \\ \frac{dV}{dt} = \Psi S - \lambda_V V, \\ \frac{dD}{dt} = \alpha_1(I_w + P_w) + \alpha_2(I_m + P_m) + \alpha_H H, \\ \frac{dW}{dt} = \eta_1(I_w + P_w) + \eta_2(I_m + P_m) - K_w W. \end{cases} \tag{2.6}$$

where

$$\lambda_S = \frac{\beta_w W}{1 + \alpha_w W} + \frac{\beta_1 c(t)(I_w + P_w)}{N} + \frac{\beta_2 c(t)(I_m + P_m)}{N},$$
$$\lambda_V = \frac{\theta\beta_w W}{1 + \alpha_w W} + \frac{\theta\beta_1 c(t)(I_w + P_w)}{N} + \frac{\theta\beta_2 c(t)(I_m + P_m)}{N},$$
$$h(t) = \frac{(H_c - H)}{P_w + P_m}.$$

Here the contact rate is denoted by $c(t)$ and the per-act transmission probability in contact with I_w (resp. I_m) and P_w (resp. P_m) is β_1 (resp. β_2). And the term β_w describes the indirect transmission rate at which the susceptible individuals (S) or vaccinated individuals (V) gets infected with the virus in the environments (W). Note that health experts and government have been advising the public to minimize contacts with infectious individuals as much as possible during the outbreak. It follows that the increasing rate of the number of infected individuals caused by indirect transmission decreases as the viral load in the environments increases. Therefore in our model we propose new infections through

indirect transmission occur in the form $\frac{\beta_w SW}{1+\alpha_w W}$, $\frac{\theta\beta_w VW}{1+\alpha_w W}$, where $\frac{1}{1+\alpha_w W}$ reflects an inhibition effect resulting from the reducing contact rate as the density of virus in the environment increases, α_w is called the saturation coefficient, θ denotes the ratio of the probability at which the vaccinated individuals V is infected compared with the susceptible individuals S. A susceptible (S) or vaccinated individual (V) may be infected by a SARS-CoV-2 strain (either the wild or the mutant) through direct transmission and entered a latent infection stage (E), where infections occur in the form $\frac{\beta_1 c(t)S(I_m+P_m)}{N}$, $\frac{\beta_2 c(t)S(I_w+P_w)}{N}$, $\frac{\theta\beta_1 c(t)V(I_w+P_w)}{N}$, $\frac{\theta\beta_2 c(t)V(I_m+P_m)}{N}$. Undergoing a mean incubation of $\frac{1}{\sigma}$ days, q proportion of infected individuals progressed into the infecteds with mutant strains (I_m), $1-q$ proportion of infected individuals progressed into the infecteds with wild strains (I_w). In model (2.6), $\delta(t)$ denotes the diagnosis rate for infected individuals, α_1, α_2 and $\alpha_H(t)$ denote the disease-induced death rates for I_w, P_w, I_m, P_m and H, respectively, $\frac{H_c-H}{P_w+P_m}$ denotes the hospitalization rate, γ_1, γ_2 and $\gamma_H(t)$ are the recovery rates for I_w, P_w, I_m, P_m and H, respectively. Note that those individuals confirmed with COVID-19 may not be hospitalized due to the shortage of hospital beds, so whether the confirmed individuals could be hospitalized or not depends on the daily number of empty hospital beds. If the hospital beds are insufficient, only a part of the confirmed individuals ($H_c(t) - H$) could be hospitalized, where $H_c(t)$ denotes the number of hospital beds at time t in India, taking the form derived from the logistic model (1). See more detailed definitions and values of variables and parameters listed in Table 1.

To fit our targeted model to the data, we initially analyzed the data to set the initial values for the state variables. According to the news reports, 1,500,000 Indian health workers and frontline workers had received at least one dose of COVID-19 vaccine as of March 1, 2021, so we set $V(0) = 15,000,000$. During the initial stage of the second wave of COVID-19 outbreak in India, all the Indians, with a total population of 1,354,051,854, except the vaccinated and infected individuals (the cumulative number of infecteds was 11,123,619 as of 1 March 2021) were susceptible to the virus, so direct calculation yields $S(0) = 1,327,100,000$. We assumed that all the previously infected individuals were either recovered (the cumulative number of recovereds was 10,796,558), dead (the cumulative number of deaths was 157,275) or received treatment in the hospital till 1 March, 2021, so we derived the initial value of hospitalized individuals $H(0) = 14,786$. On March 1, 2021, the daily number of recovered individuals was 11,990, so we set $R(0) = 11,990$. All other parameters and variables were estimated or from the reference.

We next conducted data fitting using our targeted model to estimate the values of the parameters. There are generally three parameter estimation methods, i.e., least square method, maximum likelihood estimation method, and Bayesian estimation method. It is necessary to define the maximum likelihood function in advance when we adopt the maximum likelihood estimation method to estimate parameters. The prior probability density of the estimated parameters should be determined in advance if we will estimate the parameters using the Bayes estimation method. When the least square method is chosen to estimate parameters, we do not need prior statistical characteristics, so it is easier to solve and is widely used. Compared with other parameter estimation methods, the unknown parameters can be easily obtained by using the least square method, and the sum of squares of errors between the obtained data and the actual data is minimized [48]. The nonlinear least-square method is carried out in MATLAB, using the command fmincon, which is a part of the optimization toolbox in MATLAB and finds a constrained minimum of a function of several variables. So in the following, we used the

Table 1. Estimated initial values of variables and parameters for model (2.6).

Variables		Description	Initial value	Resource
S		Susceptible population	1,327,100,000	Data
E		Exposed population	500,000	LS
I_w		Infected population with the wild strain	120,000	LS
I_m		Infected population with the mutant strain	180,000	LS
P_w		Confirmed with the wild strain but not hospitalized population	60,000	LS
P_m		Confirmed with the mutant strain but not hospitalized population	95,000	LS
H		Confirmed and hospitalized population	14,786	Data
R		Recovered population	11,990	Data
W		Density of virus in the contaminated environments	200,000	LS
V		Vaccinated population	15,000,000	Data
Parameters		**Description**	**Value**	**Resource**
β_1		The per-act transmission probability in contact with I_w and P_w	0.0288	LS
β_2		The per-act transmission probability in contact with I_m and P_m	0.06	LS
β_w		Indirect transmission rate	5.5576×10^{-4}	LS
α_w		Saturation coefficient	0.0983	LS
	c_0	Contact rate before 9 April	10.2678	LS
$c(t)$	c_1	Minimum contact rate with control strategies	4.0027	LS
	r_c	Exponential decreasing rate of the contact rate	0.6352	LS
Ψ		Vaccination rate for susceptible individuals	0.0941	LS
θ		Ratio of the probability of V being infected compared with S	0.1878	LS
q		Proportion of infected individuals with the mutant strain	0.5957	LS
σ		Progression rate of exposed individuals to infectives	1/4.003	LS
	δ_0	Initial diagnose rate of infected individuals	0.1214	LS
$\delta(t)$	δ_1	Maximum diagnose rate of infected individuals	0.6458	LS
	δ_2	Final diagnose rate of infected individuals	0.1997	LS
	r_δ	Exponential decreasing rate of diagnose rate	8.0101	LS
	H_{c0}	Initial number of hospital beds for COVID-19 in India	35000	LS
$H_c(t)$	r	Net increasing rate of hospital beds	0.09	LS
	M	Maximum capacity of hospital beds	1700000	LS
	γ_{H0}	Initial Recovery rate of confirmed individuals	0.3306	LS
$\gamma_H(t)$	γ_{H1}	Maximum Recovery rate of confirmed individuals	0.3402	LS
	γ_{H2}	Final Recovery rate of confirmed individuals	0.021	LS
	r_H	Exponential increasing rate of recovery rate	0.0745	LS
γ_1		Recovery rate of the infecteds and confirmed individuals with the wild strain before hospitalization	0.09871	[49]
γ_2		Recovery rate of the infecteds and confirmed individuals with the mutant strain before hospitalization	0.096	LS
α_1		Disease-induced death rate of the infecteds and confirmed individuals with the wild strain before hospitalization	2.92×10^{-5}	LS
α_2		Disease-induced death rate of the infecteds and confirmed individuals with the mutant strain before hospitalization	3.6786×10^{-5}	LS
	α_{H0}	Minimum disease-induced death rate of hospitalized individuals	0.004	LS
$\alpha_H(t)$	α_{H1}	Reduced disease-induced death rate of hospitalized individuals	0.0039	LS
	α_{H2}	Final disease-induced death rate of hospitalized individuals	3.2485×10^{-4}	LS
	r_α	Exponential decreasing rate of disease-induced death rate	0.0815	LS
η_1		The virus shedding rate from the infecteds and the confirmed individuals with wild strain	3.98×10^{-4}	[49]
η_2		The virus shedding rate from the infecteds and the confirmed individuals with mutant strain	4×10^{-4}	LS
K_w		The clearance rate of the virus	0.01	[49]

nonlinear least-square method to validate our targeted model. The objective function is

$$f(\Theta) = \sum_{k=1}^{k=n} (\tilde{C}(T_k) - C(T_k))^2 + \sum_{k=1}^{k=n} (\tilde{R}(T_k) - R(T_k))^2 + \sum_{k=1}^{k=n} (\tilde{D}(T_k) - D(T_k))^2 \tag{2.7}$$

where Θ is the vector of parameters to be estimated, n is the length of the epidemic data period. Here $n = 215$ since we used data from 1 March to 1 October, lasting for 215 days. T_k is the corresponding date of the $k - th$ day since 1 March 2021. $\tilde{C}(T_k), \tilde{R}(T_k), \tilde{D}(T_k)$ are the actual reported daily number of confirmed cases, recovered cases and deaths on the date T_k, respectively. $C(T_k), R(T_k), D(T_k)$ are the estimated daily number of confirmed cases, recovered cases and deaths on the date T_k, respectively. The dynamics of $C(t), R(t), D(t)$ are governed by

$$\begin{cases} \dfrac{C(t)}{dt} = h(t)(P_w(t) + P_m(t)), \\ \dfrac{R(t)}{dt} = \gamma_H(t)H, \\ \dfrac{D(t)}{dt} = \alpha_H(t)H. \end{cases} \tag{2.8}$$

where $P_w(t), P_m(t)$ and $H(t)$ are determined by model (2), $h(t), \gamma_H(t)$ and $\alpha_H(t)$ are as defined above.

3. Results

• *Parameter estimation and model fitting*

By fitting our targeted model to the data of the daily number of confirmed cases, recovered cases and deaths from 1 March to 1 October, 2021, we have obtained the estimated values of the unknown parameters. The fitting result of the targeted model (2) to the epidemic data was shown in Figure 3(a)–(c). The estimated values of unknown parameters and initial conditions of variables and parameters are reported in Table 1. In Figure 3, the red circles represent the data from 1 March to 1 October, 2021, the best-fitting results of the daily number of confirmed cases, recovered cases and deaths are plotted in black solid lines, showing that our targeted model captures the data well.

Note that the data we used to fit the model, including the daily number of confirmed cases, recovered cases and deaths, are not highly linearly correlated, and there are very few outliers in the data, so the least square method used in this paper is stable. In addition, in order to improve the stability of parameter estimation adopted in this work, we selected a relatively large amount of data, i.e., 215 days of data, for fitting. In fact, the parameter estimation in this work was difficult. On the one hand, there were many parameters needed to be estimated; on the other hand, some of the parameters were piece-wise defined or time-dependent, which increased the difficulty in parameter estimation. In addition, the magnitude of the data on the second wave of COVID-19 epidemic in India was relatively large, and the error between the reported data and the actual situation was also relatively large, which also increased the difficulty of parameter estimation. Nevertheless, we have provided a good estimate, as shown in Figure 3.

To further validate the targeted model, we compared the actual data and estimates on the cumulative number of confirmed cases, recovered cases and deaths from 1 March to 1 October, 2021, as shown in Table 2. Table 2 shows that the estimated value of the cumulative number of confirmed cases is

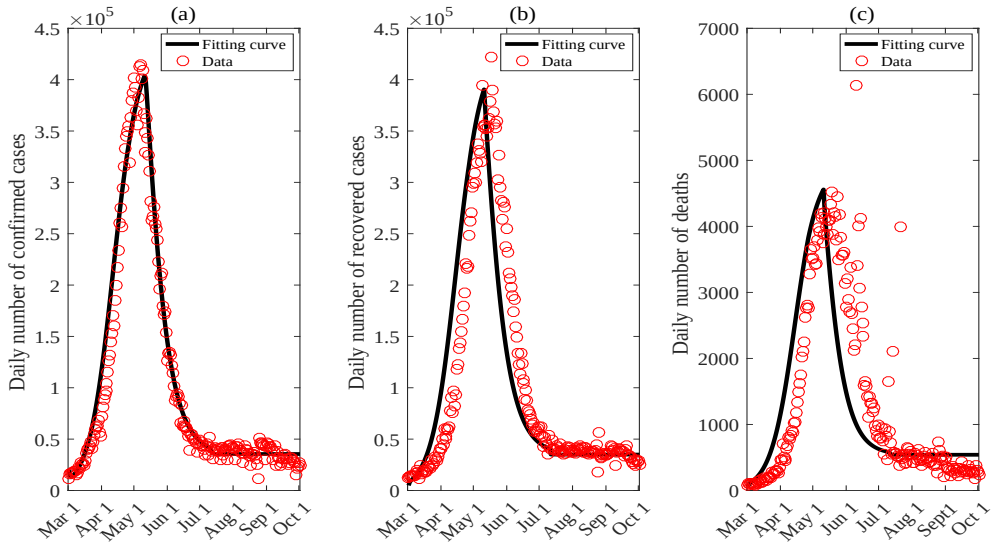

Figure 3. Fitting result for the data from 1 March to 1 October, 2021 in India. (a) Fitting of daily number of confirmed cases; (b) fitting of daily number of recovered cases; and (c) fitting of daily number of deaths. The red circles represent the reported data, the black curves are the best fitting curves of model (2) to the data.

Table 2. Data on cumulative number of confirmed cases, recovered cases and deaths versus the estimates from 1 March to 1 October.

	Data	Estimated value	Proportion in the whole or infected population (data)	Proportion in the whole or infected population (estimated)
Cumulative number of confirmed cases	22,677,342	24,123,250	1.674%	1.782%
Cumulative number of recovered cases	22,276,412	22,194,430	98.232%	92.004%
Cumulative number of deaths	291,410	272,607	1.285%	1.130%

6% higher than the actual data, i.e., 1,445,908 more cases. The estimated values on the cumulative number of recovered cases (resp. deaths) are 0.4% (resp. 6%) lower than the actual data, i.e., 81,982 less recovered cases (resp. 18,803 less deaths). Note that in order to fit the data on the death used in this paper, the number of deaths here is only those died in the hospital. The proportion in the first row of Table 2 refers to the proportion of the cumulative number of confirmed cases in the total population; while that in the second (resp. third) row refers to the proportion of the cumulative number of recovered cases (resp. deaths) in the confirmed population. We observe that the errors between the estimated value and the actual data of these three ratios are small, i.e., 0.108, 6.228 and 0.155%, respectively. In Table 3, we compared the peak size of the data on the daily number of confirmed cases, recovered cases and deaths with the estimated ones. We found that the peak size of the data on the daily number of confirmed cases was 10,593 larger than that of the estimated value, with a relative error 2.556%. The peak size of the data on the daily number of deaths was 34 smaller than that of the estimated value, with a relative error 0.760%. In Table 4, we compared the time of the data when the daily number of confirmed cases less than 50,000 and that when the daily number of deaths less than

Table 3. Comparison of actual and estimated daily numbers of confirmed cases, recovered cases and deaths at peak from 1 March to 1 October 1.

	Peak size (data)	Peak size (estimated)	Absolute error	Relative error
Daily number of confirmed cases	414,433	403,840	10,593	2.556%
Daily number of recovered cases	422,394	390,570	31,824	7.534%
Daily number of deaths	4525	4559	34	0.760%

Table 4. Comparison of actual and estimated time when the daily number of confirmed cases or deaths less than 50,000 or 600.

	Date (data)	Date (estimated)
Time when the daily number of confirmed cases less than 50000	25 June	29 June
Time when the daily number of deaths less than 600	12 July	5 July

600. We found that the estimated time when the daily number of confirmed cases less than 50,000 is 4 days later than the that in the data; the estimated time when the daily number of deaths less than 600 is 7 days earlier than that in the data. As a result, our targeted model fitted the data well and it was reliable.

We calculated the basic reproduction number by using the next generation matrix method [50]. Denoting $Z \equiv (E, I_w, I_m, P_w, P_m, W)$, we had $\dot{Z} = G(Z)$. Let $G(Z) = \mathcal{F} + \mathcal{V}$, where $\mathcal{F}$ represent the vector of new infections and $\mathcal{V}$ represent the vector of all other transitions, respectively. And we get

$$\mathcal{F} = \begin{bmatrix} \frac{\beta_w S W}{1+\alpha_w W} + \frac{\beta_1 c(t) S (I_w + P_w)}{N} + \frac{\beta_2 c(t) S (I_m + P_m)}{N} + \frac{\theta \beta_w V W}{1+\alpha_w W} + \frac{\theta \beta_1 c(t) V (I_w + P_w)}{N} + \frac{\theta \beta_2 c(t) V (I_m + P_m)}{N} \\ 0 \\ 0 \\ 0 \\ 0 \\ 0 \end{bmatrix},$$

$$\mathcal{V} = \begin{bmatrix} \sigma E \\ (\delta(t) + \alpha_1) I_w - (1-q)\sigma E \\ (\delta(t) + \alpha_2) I_m - q\sigma E \\ (h(t) + \gamma_1 + \alpha_1) P_w - \delta(t) I_w \\ (h(t) + \gamma_2 + \alpha_2) P_m - \delta(t) I_m \\ K_w W - (\eta_1 (I_w + P_w) + \eta_2 (I_m + P_m)) \end{bmatrix}.$$

Differentiating $\mathcal{F}$ and $\mathcal{V}$ with respect to Z and computing them at the initial state give

$$F = \begin{bmatrix} 0 & \frac{\beta_1 c(t) S_t + \theta\beta_1 c(t) V_t}{N_t} & \frac{\beta_2 c(t) S_t + \theta\beta_2 c(t) V_t}{N_t} & \frac{\beta_1 c(t) S_t + \theta\beta_1 c(t) V_t}{N_t} & \frac{\beta_2 c(t) S_t + \theta\beta_2 c(t) V_t}{N_t} & \frac{\beta_w S_t + \theta\beta_w V_t}{(1+\alpha_w W_t)^2} \\ 0 & 0 & 0 & 0 & 0 & 0 \\ 0 & 0 & 0 & 0 & 0 & 0 \\ 0 & 0 & 0 & 0 & 0 & 0 \\ 0 & 0 & 0 & 0 & 0 & 0 \\ 0 & 0 & 0 & 0 & 0 & 0 \end{bmatrix},$$

$$V = \begin{bmatrix} \sigma & 0 & 0 & 0 & 0 & 0 \\ -(1-q)\sigma & \delta(t)+\alpha_1 & 0 & 0 & 0 & 0 \\ -q\sigma & 0 & \delta(t)+\alpha_2 & 0 & 0 & 0 \\ 0 & -\delta(t) & 0 & h(t)+\gamma_1+\alpha_1 & 0 & 0 \\ 0 & 0 & -\delta(t) & 0 & h(t)+\gamma_2+\alpha_2 & 0 \\ 0 & -\eta_1 & -\eta_2 & -\eta_1 & -\eta_2 & K_w \end{bmatrix}.$$

Then the effective reproduction number can be approximately defined as

$$R_e(t) = \rho(FV^{-1}) = R_e^s(t) + R_e^w(t), \tag{3.1}$$

where $R_e^s(t)$ and $R_e^w(t)$ denote the effective reproduction numbers of direct transmission and indirect transmission, respectively, and

$$\begin{aligned} R_e^s(t) =& \frac{(1-q)\beta_1 c(t)(S_t+\theta V_t)}{N_t(\delta(t)+\alpha_1)} + \frac{(1-q)\delta(t)\beta_1 c(t)(S_t+\theta V_t)}{N_t(\delta(t)+\alpha_1)(h(t)+\gamma_1+\alpha_1)} + \frac{q\beta_2 c(t)(S_t+\theta V_t)}{N_t(\delta(t)+\alpha_2)} + \\ & \frac{q\delta(t)\beta_2 c(t)(S_t+\theta V_t)}{N_t(\delta(t)+\alpha_2)(h(t)+\gamma_2+\alpha_2)}, \\ R_e^w(t) =& \left[\frac{(1-q)\eta_1(\delta(t)+h(t)+\gamma_1+\alpha_1)}{(\delta(t)+\alpha_1)(h(t)+\gamma_1+\alpha_1)} + \frac{q\eta_2(\delta(t)+h(t)+\gamma_2+\alpha_2)}{(\delta(t)+\alpha_2)(h(t)+\gamma_2+\alpha_2)}\right]\frac{\beta_w(S_t+\theta V_t)}{(1+\alpha_w W_t)^2 k_w}. \end{aligned}$$

According to the reported values of the parameters and initial conditions, we get the estimated effective reproduction number, as shown in Figure 4, where the grey region indicates the lockdown period, i.e., from 9 April to 31 May, 2021. It follows from Figure 4 that the effective reproduction number $R_e(t)$ falls below the threshold of 1 since 9 April when the lockdown strategy was implemented. And the effective reproduction number is relatively small during the lockdown, i.e., from 9 April to 31 May, 2021 when the public was not allowed to go out except for essential activities such as buying daily necessities and seeking medical treatment. Note that a slight rebound occurred on 31 May, 2021 when the lockdown strategy was suspended. It follows that the outbreak becomes controllable since the implementation of lockdown.

• *Uncertainty and sensitivity analysis*

Considering the uncertainty of the model parameters, we conducted sensitivity analysis of the effective reproduction number $R_e(t)$ with respect to various parameters over time by computing the partial

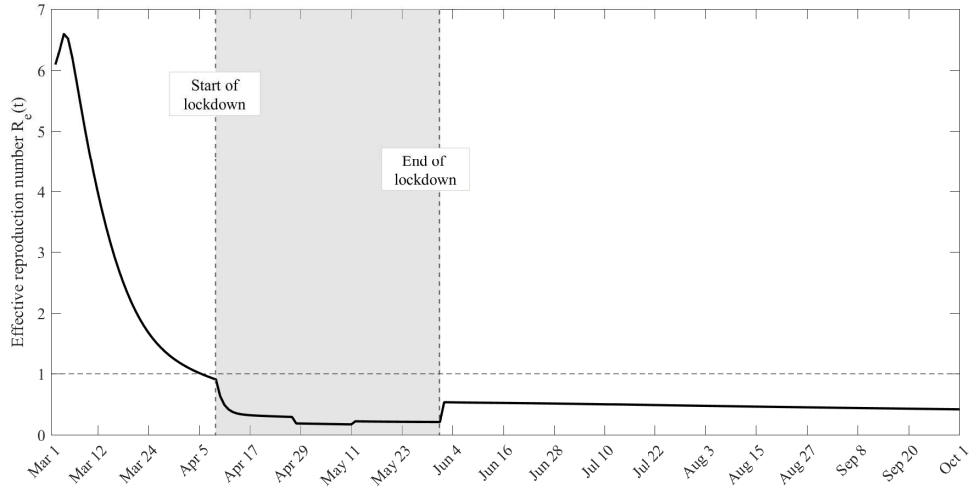

Figure 4. Estimated effective reproduction number from 1 March to 1 October, 2021 in India.

rank correlation coefficients (PRCCs) based on Latin Hyperbolic Sampling [51]. We chose the parameters closely related to the epidemic transmission and containments including the parameters related to the evolution of contact rate (c_0), proportion of infected individuals with the mutant strain (q), vaccination rate for susceptible individuals (Ψ), ratio of the probability of the vaccinated population being infected compared with the susceptible population (θ), initial diagnose rate of infected individuals (δ_0), the per-act transmission probability in contact with I_m and P_m (β_2), net increasing rate of hospital beds (r), maximum capacity of hospital beds(M), with other parameters fixed, as shown in Figure 5. The monotonic relationship between the outcomes of effective reproduction number $R_e(t)$ and each

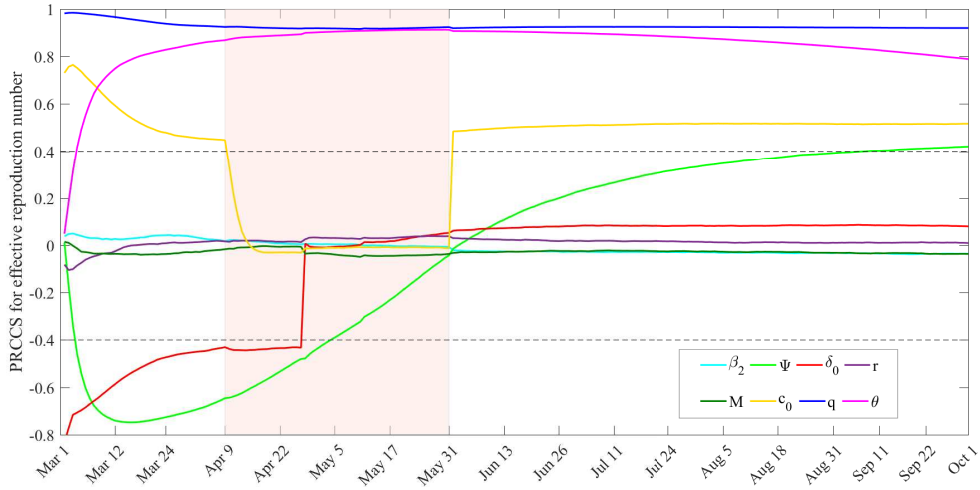

Figure 5. Partial rank correlation coefficients (PRCCs) of the effective reproduction number ($R_e(t)$) for $\beta_2, \Psi, \delta_0, r, M, c_0, q, \theta$ from 1 March to 1 October, 2021 in India. The shadow region indicates the period of lockdown.

parameter was assessed over the entire time interval. The values of the partial rank correlation coeffi-

cients (PRCCs) of each parameter over the time interval was calculated, which allowed us to determine whether the significance of one parameter occurred during the progression of the dynamics of our targeted model. The absolute values of PRCCs greater than 0.5 were considered as indicating significant correlations between the parameters and the effective reproduction number. Figure 5 showed that the proportion of I_m (i.e., q), ratio of the probability of V being infected compared with S (i.e., θ), and initial contact rate (i.e., c_0) were positively correlated with $R_e(t)$ almost over the entire time interval, which indicated that declining q, θ and c_0 led to a significant decreasing of the effective reproduction number $R_e(t)$ over the whole time interval. The initial diagnose rate of infected individuals δ_0 was negatively correlated with $R_e(t)$ before 29 April; while the vaccination rate of S (i.e., Ψ) was negatively correlated with $R_e(t)$ before the end of lockdown. It followed that increasing the diagnose rate and vaccination rate could lead to a significant decreasing of the effective reproduction number $R_e(t)$. It was worth emphasizing that the correlation between the effective reproduction number $R_e(t)$ and the contact rate c_0 became very weak during the implementation of lockdown, which was because very little social activities occurred during the lockdown and the effective reproduction number was mainly determined by other factors. According to Figure 5, increasing the intensity of social distancing (i.e., decreasing c_0), strengthening awareness of self-protection (i.e., reducing q), vaccinating on time to improve the efficiency of vaccine protection (i.e., decreasing θ and increasing Ψ before the end of lockdown), and increasing the diagnosis rate (i.e., increasing δ_0), all could assist in containing the epidemic.

It was reported that India has crossed 300,000 COVID-19 deaths till 24 May, 2021, making it the third country after the United States and Brazil [52]. In fact, this outbreak in India crippled the health system and many people died from a shortage of medical resources. According to the report from the Global News on 20 July, 2021, most experts believed India's official toll of more than 414,000 deaths was a vast undercount although the government has dismissed these concerns [53]. The count could have missed those deaths occurring in overwhelmed hospitals or while health care was delayed or disrupted. And it was estimated that the death toll from COVID-19 in India could be nearly 10 times the deaths reported by India government, which indicates the number of COVID-19 deaths in India was far higher than that was reported. In the following, we choose the number of deaths as an index and identify the key factors affected the COVID-19 outbreak in India by exploring the impact of the factors on the number of deaths. To this end, we initially use the targeted model to estimate the total deaths in reality, including deaths with the wild strain or mutant strain before hospitalization and deaths in the hospitals. For convenience, we denote the deaths with the wild (resp. mutant) strain before hospitalization and the deaths in the hospitals as D_w (resp. D_m) and D_h in the following, respectively. The sum of the deaths with wild (D_w) or mutant strain (D_m) before hospitalization or in hospitals (D_h) is referred as total deaths in the rest of this work. We calculate the average number of deaths with the mutant (resp. wild) strain before hospitalization for each day of the weeks from 1 March to 27 September, 2021. For instance, we calculate the average number of daily deaths from 1 March to 7 March, 2021, and recorded it as the average daily number of deaths of the first week. And the average daily number of deaths of the second week is calculated in terms of the daily deaths from 8 March to 14 March, 2021. Repeating the above process, we obtain the average daily number of deaths for any week between 1 March and 1 October, 2021. We similarly calculate the average daily number of deaths in the hospitals for each week from 1 March to 1 October, 2021, as shown in Figure 6. Note that the data we used to fit our model is from 1 March to 1 October, 2021, but there is little change in the last days, so here we ignored the data of the last four days such that the remained days are exactly

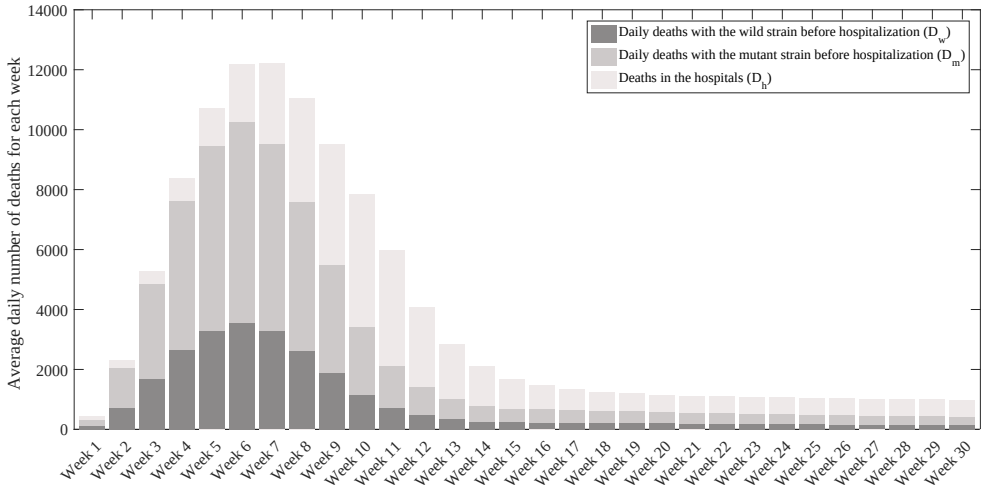

Figure 6. Average daily number of deaths for each week from 1 March to 27 September, 2021 in India. Dark grey, moderate grey and light grey bars show the average daily number of deaths with the wild strain before hospitalization (D_w), average daily number of deaths with the mutant strain before hospitalization (D_m), and average daily deaths in the hospital (D_h) for each week.

30 weeks. Figure 6 suggests that more people die from the mutant strain than from the wild strain, and more people die before hospitalization than in the hospital. It is also found that the peak time of the actual deaths is at weeks 6–7, in which days the average daily number of deaths rises up to about 12, 000, about six times the reported death toll. This is consistent with a recent study of actual deaths in COVID-19, India [54].

In the next, we quantify how the mutant strain, contaminated environments and vaccination with the shortage of medical resources affect the spread of COVID-19 in India. To this end, we choose the per-act transmission probability in contact with the infecteds with symptoms caused by mutant strain (β_2), proportion of infected individuals with the mutant strain (q), indirect transmission rate (β_w), saturation coefficient (α_w), vaccination rate (Ψ), ratio of the probability of the vaccinated population being infected compared with the susceptible population (θ), recovery rate of the infecteds and confirmed individuals with the mutant strain before hospitalization (γ_2), and disease-induced death rate of the infecteds and confirmed individuals with the mutant strain before hospitalization (α_2) to explore what would happen if these factors vary.

We first used contour plots to examine the dependence of the peak time and peak size of the daily number of total deaths in reality on β_2 and q, as shown in Figure 7. It follows from Figure 7 that reducing the proportion of infected individuals with the mutant strain q, and the per-act transmission probability in contact with the infecteds with symptoms caused by mutant strain β_2, would delay the peak time of the number of total deaths in reality (Figure 7(a)), and the peak size of the number of total deaths in reality would be lowered substantially (Figure 7(b)). We also conducted contour plotting to investigate the dependence of the peak time and peak size of the daily number of total deaths in reality on other key parameters including γ_2 and α_2 (Figure 10), β_w and α_w (Figure 11), and Ψ and θ (Figure 12). Figure 10 shows that the peak time mainly depends on the recovery rate of infected

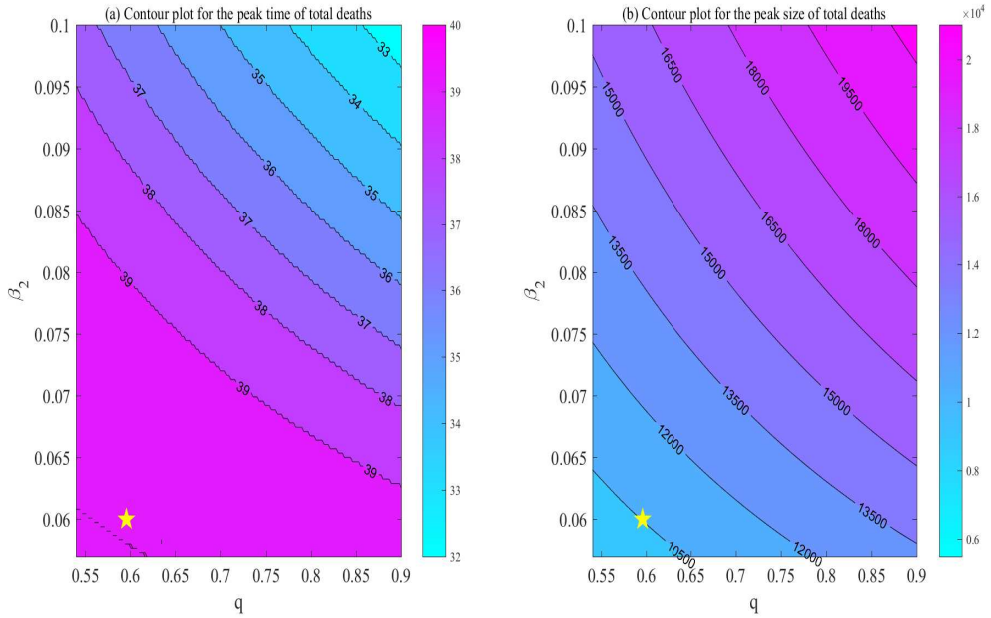

Figure 7. Contour plots of the peak time and peak size of the daily number of total deaths in reality to β_2 and q from 1 March to 1 October, 2021 in India. The yellow star demonstrates the position of (β_2, q) that we have reported in Table 1.

and confirmed individuals with the mutant strain before hospitalization γ_2; while the peak size mainly depends on the disease-induced death rate of infected and confirmed individuals with the mutant strain before hospitalization α_2. Increasing γ_2 could lead to an earlier peak time and decreasing α_2 would result in a smaller peak size. Figure 11 demonstrates that reducing the indirect transmission rate β_w while increasing the saturation coefficient α_w would lead to a delay in the peak time (Figure 11(a)) and a significant decreasing in the peak size (Figure 11(b)). A small increasing in the indirect transmission rate β_w will trigger into a significant advancing of the peak time as well as a great increasing of the peak size, which indicates a more impact of the indirect transmission rate than the saturation coefficient α_w on the peak time and peak size of the total deaths. Figure 12 demonstrates that the ratio of the probability of the vaccinated population being infected θ has a more significant impact on the peak time compared with the vaccination rate Ψ; while the vaccinate rate Ψ has a greater effect on the peak size compared with θ. As a result, Figures 7–12 demonstrate that reducing the proportion of infected individuals with the mutant strain q, the transmission probability of mutant strain β_2, the disease-induced death rate caused the mutant strain α_2, or the vaccination rate, all could alleviate the outbreak by diminishing the peak size of the daily number of total deaths in reality.

To further explore the exact impact of the mutant strain on the COVID-19 outbreak in India, we investigated how the daily deaths with the wild strain (D_w), the mutant strain (D_m) and the sum of daily deaths before hospitalization (i.e., the sum of D_w and D_m, which we denote as $D_w + D_m$ in the rest) vary with different values of the per-act transmission probability in contact with the infecteds with symptoms caused by mutant strain (β_2) and the proportion of infected individuals with the mutant strain (q). We conducted a sensitivity analysis to show what would happen if β_2 was increased by 20, 50, 80%, q was increased to 0.7, 0.8, 0.9, as shown in Figure 8(a)–(d). It follows that increasing

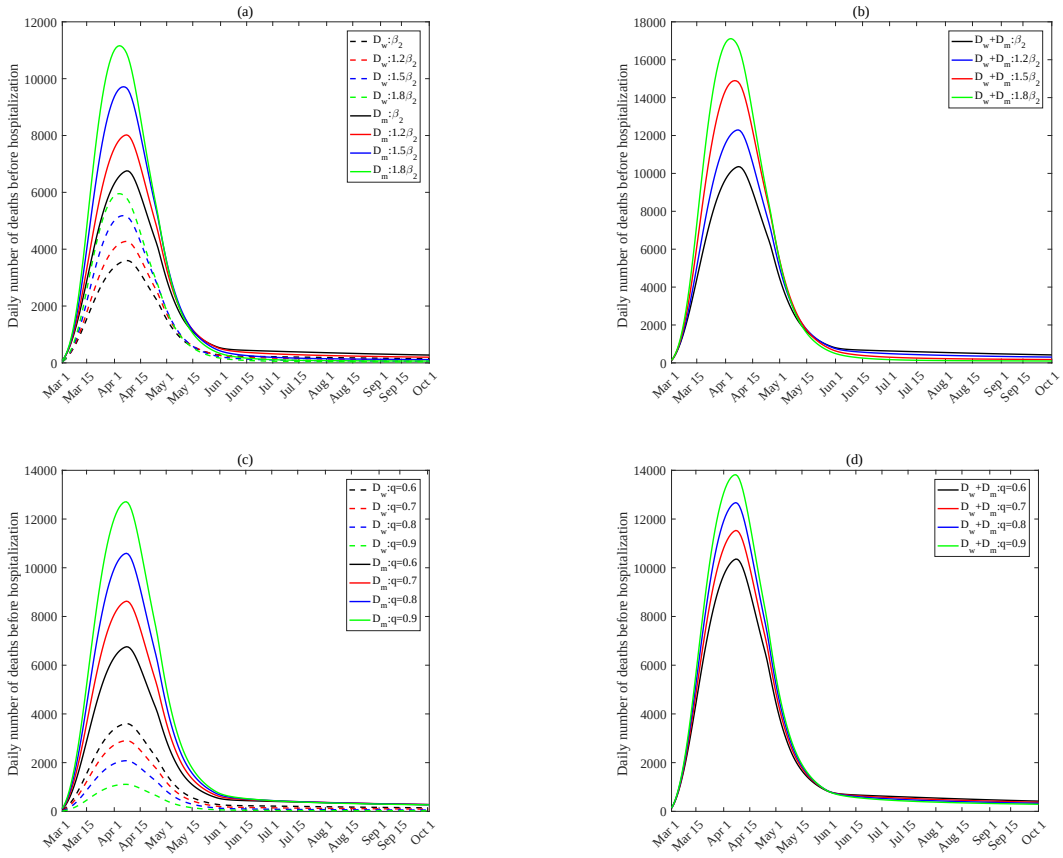

Figure 8. Variation of the daily deaths before hospitalization with different values of β_2 and q from 1 March to 1 October, 2021 in India, where D_w and D_m represent daily deaths with the wild strain and the mutant strain, $D_w + D_m$ represents the sum of the daily deaths with the wild and mutant strains.

the per-act transmission probability in contact with the infecteds with symptoms caused by mutant strain (β_2), or the proportion of infected individuals with the mutant strain (q), both could lead to an increasing of the average daily deaths with the wild or mutant strain before hospitalization (D_w or D_m). We also explored the variation of the daily deaths with the wild strain (D_w), the mutant strain (D_m) and the sum of them ($D_w + D_m$) as the recovery rate and disease-induced death rate of the infecteds and confirmed individuals with the mutant strain before hospitalization (γ_2 and α_2) varied. We analyzed what would happen when the recovery rate of the infecteds and the confirmed individuals with the mutant strain before hospitalization (γ_2) was increased by 20, 50, 80% while the disease-induced death rate of the infecteds and the confirmed individuals with the mutant strain before hospitalization (α_2) was declined by 20, 40, 60%, respectively, as shown in Figure 13(a)–(b). They demonstrated that increasing γ_2 while decreasing α_2 would lead to the decline of the daily deaths with the wild strain and mutant strain before hospitalization (D_w and D_m). It's worth emphasizing that increasing γ_2 while decreasing α_2 had a more significant decline on the daily deaths with mutant strain than that on the daily deaths with the wild strain. We found that the mutant strain played a vital role in the outbreak of the epidemic. A significant increasing of the daily deaths would occur if the transmission

probability (β_2) or the proportion (q) was raised; while a great decreasing would happen on the daily deaths if the the recovery rate (γ_2) was increased with a decline of the disease-induced death rate (α_2). We further investigated the impact of vaccination rate (Ψ), vaccine effectiveness ($1-\theta$) and the indirect transmission rate of the contaminated environments (β_w) on the daily deaths with the wild strain or mutant strain (D_w or D_m) or the sum of daily deaths before hospitalization ($D_w + D_m$). We conducted a sensitivity analysis to examine the variation of D_w, D_m and D_h if Ψ, θ or β_w were raised by 20 50, 80%, respectively, as shown in Figure 13. It follows from Figure 13 that increasing the vaccination rate or the rate of the probability of infection in a vaccinated individual would trigger a significantly decreasing or increasing of the daily deaths before hospitalization, as shown in Figure 13(c)–(f). If the indirect transmission rate was raised to $1.2\beta_w$, $1.5\beta_w$ and $1.8\beta_w$, the daily deaths with the wild strain, mutant strain or the total deaths before hospitalization increases although it is not very obvious. We found that the vaccination strategy had a more significant effect than the environmental transmission on the spread of the epidemic. A noteworthy decreasing of the daily deaths occurred if the vaccination rate (Ψ) or vaccine effectiveness ($1-\theta$) was raised. In order to better understand the effect of the mutant strain on the epidemic, we further examined the variation of the total deaths in reality as the key parameters (β_2, q) vary. We calculated the average daily number of total deaths, including deaths with the wild strain (D_w), mutant strain (D_m) before hospitalization and the deaths in the hospital (D_h), for very two weeks between 1 March to 27 September, 2021, as shown in Figure 9. It follows from Figure 9(a) and (b) that increasing the per-act transmission probability in contact with

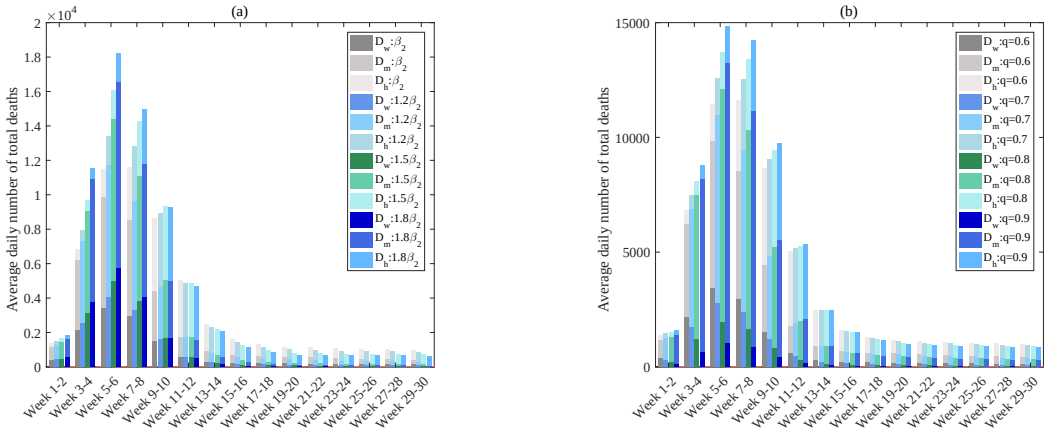

Figure 9. Impact of the mutant strain (β_2, q) on the total deaths in reality from 1 March to 27 September, 2021 in India. Dark grey, cyan, green and blue represent the average daily deaths with the wild strain before hospitalization (D_w); moderate grey, cyan, green and blue stand for the average daily deaths with the mutant strain before hospitalization (D_m); light grey, cyan, green and blue represent the average daily deaths in the hospital (D_h) every two weeks.

the infecteds with symptoms caused by mutant strain (β_2) and the proportion of infected individuals with the mutant strain (q), both could result in a great increasing of the total number of deaths in reality. To highlight the effect of the environmental transmission and vaccination on the epidemic, we calculated the average daily number of total deaths in reality as the key parameters ($\gamma_2, \alpha_2, \Psi, \theta, \beta_w$) varied, as shown in Figure 14. We can easily obtained from Figure 14 (c) that increasing the ratio of the probability of the vaccinated individuals being infected (θ) could result in a great increasing

of the total number of deaths in reality. Figure 14(a) and (b) showed that increasing the recovery rate of the infecteds and the confirmed individuals with the mutant strain before hospitalization (γ_2) while decreasing the disease-induced death rate of the infecteds and the confirmed individuals with the mutant strain before hospitalization (α_2), or raising the vaccination rate (Ψ), both could lead to a decreasing of the total number of deaths. It can be seen from Figure 14(d) that an increase in the indirect transmission rate (β_w) could lead to a slight increase in the total number of deaths. It is worth noting that all of these factors have a strong influence on the total number of deaths in the early stage of the outbreak, such as during the early eight weeks; while only a very weak effect on the total number of deaths in the late stage of the outbreak, such as during the period through week 11 to week 30. This was because during the later stage of the epidemic, Indian government implemented a lot of containments including lockdown and other control measures to stop the further spread, and the assistance of medical resource from other countries reduced the death toll. The mutant strain and vaccination, besides the contaminated environments, had a more significant effect on the deaths with the mutant strain before hospitalization than they on the deaths with the wild strain before hospitalization. The number of deaths in the hospitals was very little affected by these factors compared to the number of deaths before hospitalization. The findings demonstrate that the vaccination strategy and the environmental transmission have an obvious impact on the transmission of the epidemic, especially during the early stage. The vaccination strategy (resp. environmental transmission) could alleviate (resp. aggravate) the outbreak by decreasing (resp. increasing) the total deaths.

4. Discussion and conclusions

• *Discussion*

Since the starting of the COVID-19 pandemic in early 2020, countries worldwide are devoted to finding effective containments to halt the number of cases and deaths. India, as one of the countries with very high population density, has experienced multiple waves of COVID-19 although they have always been struggling to curb the outbreak. The second wave of COVID-19 in India has had a heavy blow to the country, although vaccine distribution had already commenced in India. There are many a factor, including the more pathogenic mutant strain than the wild one, the contaminated environments and the serious shortage of medical resources, that triggered this outbreak. Quantification of the effect of these factors and the public health mitigation programs, including vaccination and implementation of lockdown, on the containment of the outbreak, are, thus, needed. We have done a retrospective study to quantify how these factors, together with the gradually strengthening of the nonpharmaceutical interventions (NPIs) affect the spread of COVID-19. In this work, we have proposed a nonsmooth compartment epidemic model that incorporated direct and indirect transmission as the potential transmission pathways of COVID-19. The model also mimicked the shortage of medical resources, the prevalence of mutant strains and the implementation of vaccination.

We assumed the key control parameters are time dependent and piecewise defined due to the strengthening of prevention and control measures including the implementation of lockdown strategy on 9 April, 2021, the arriving of the first batch of medical aid from UK on 27 April, the arriving of the last batch of medical aid from China on 10 May, and the gradually lifting of the containment measures on 31 May. By using the nonlinear least-square method to fit our targeted model, these time-dependent parameters and other model parameters are estimated, as reported in Table 1. The fitting

results shown in Figure 3 illustrated that the targeted model captured the data, including the daily number of confirmed cases, recovered cases and deaths well. The estimated effective reproduction number is much smaller during the implementation of lockdown than that in other time, as shown in Figure 4, which highly support the policy of lockdown. The PRCCs of the effective reproduction number $R_e(t)$ with respect to the key parameters over time indicated that reducing the proportion of infecteds with mutant strain (q), probability of vaccinated individuals being infected (θ), and initial contact rate (c_0), all could significantly decline $R_e(t)$, as shown in Figure 5. It follows that decreasing the proportion of mutant strain, infection probability of the vaccinateds, or the contact rate, all could aid in controlling the outbreak.

To reveal the vital role of the multiple factors including the mutant strain, contaminated environments and vaccination with the medical-resource constraints in the transmission of the COVID-19 in India, we chose the number of deaths as an index and explored what would happen as these factors varied. We gave an estimate of the deaths with wild strain or mutant strain before hospitalization as well as the deaths in the hospital. It revealed that there were more deaths before hospitalization than in the hospital and more people were dying from the mutant strain than from the wild strain among the deaths before hospitalization. Our sensitivity analysis showed that increasing the transmission probability of the mutant strain (β_2) and the proportion of the infecteds with mutant strain (q) could bring forward the peak time of the number of total deaths and raise the peak size, as shown in Figure 7. A slight increasing of the indirect transmission rate (β_w) could result in a significant advancing of the peak time as well as a great increasing of the peak size, shown in Figure 11. The probability of the vaccinated individuals being infected (θ) has a more significant effect on the peak time compared with the vaccination rate Ψ; while the vaccination rate (Ψ) has a greater impact on the peak size than the probability of the vaccinated individuals being infected (θ), as shown in Figure 12. The main findings demonstrate that the mutant strain and the contaminated environment trigger a significant increasing of the peak size; while the vaccination strategy leads to an obvious decreasing of the peak size.

To better understand how the multiple factors affect the second wave of the COVID-19 in India, we further explored the variation of the number of deaths with wild strain or mutant strain before hospitalization or deaths in the hospital as these factors varied, shown in Figures 8, 9, 13 and 14. We observed from these Figures that the number of deaths with mutant strain (D_m) or wild strain before hospitalization (D_w) or the deaths in the hospital (D_h) increased significantly if the transmission probability of the mutant strain (β_2), the proportion of infecteds with the mutant strain (q), or the infection probability of the vaccinated individuals (θ) was increased. We also obtained that D_m, D_w and D_h declined obviously if the recovery rate of infecteds with the mutant strain (γ_2) was increased while their disease-induced death rate (α_2) was declined, or the vaccination rate (Ψ) was raised. An increase in the indirect transmission rate (β_w) would trigger a small increase in the number of deaths with mutant strain or wild strain before hospitalization or the deaths in the hospital. The prevalence of the mutant strain and implementation of vaccination besides the contaminated environments have a strong effect on the total number of deaths in the early stage of the outbreak while they have only a very weak effect in the late stage of the outbreak. All these factors have a more significant influence on the deaths with the mutant strain than the influence they have on the deaths with the wild strain. And they have a very small influence on the deaths in the hospital. The main results show that reducing the prevalence of the mutant strain, strengthening vaccination, and increasing the virus clearance rate in the contaminated environment can effectively inhibit the spread of the epidemic, especially in the

initial stage of the outbreak.

To present a complete demonstration of the impact of the key factors mentioned in this work on the COVID-19 epidemic in India in 2021, we used the number of deaths in reality as an indicator and examined the impact of different factors on the number of deaths in the following, as shown in Table 5, where the death referred to the cumulative number of deaths in India from March 1 to October 1,

Table 5. Impact of key factors on the death toll of COVID-19 from 1 March to 1 October, 2021 in India.

Factors		Deaths with the wild strain before hospitalization (10^3)	Deaths with the mutant strain before hospitalization (10^3)	Total deaths in reality (10^3)	Death rate
Baseline values		182.089	343.316	797.473	3.306%
Mutant strain	$1.2\beta_2$	201.643	380.167	853.877	3.540%
	$1.5\beta_2$	226.329	426.653	925.054	3.835%
	$1.8\beta_2$	245.108	461.997	979.165	4.059%
	$q = 0.7$	141.972	423.804	837.840	3.473%
	$q = 0.8$	98.822	505.544	876.434	3.633%
	$q = 0.9$	51.409	591.242	914.729	3.792%
Vaccination	1.2Ψ	171.164	322.753	765.982	3.175%
	1.5Ψ	160.070	301.871	734.007	3.043%
	1.8Ψ	153.138	288.824	714.028	2.960%
	1.2θ	204.244	385.107	861.420	3.571%
	1.5θ	229.941	433.537	935.540	3.878%
	1.8θ	248.320	468.132	988.523	4.098%
Environmental transmission	$1.2\beta_w$	192.473	362.878	827.413	3.430%
	$1.5\beta_w$	204.906	386.299	863.279	3.579%
	$1.8\beta_w$	214.705	404.756	891.530	3.696%
Contact tracing	30%	154.203	290.751	717.558	2.975%
	50%	137.135	258.568	668.311	2.770%
	70%	121.624	229.318	623.548	2.585%

2021, 10^3 denoted every number should be multiplied by 10^3. Table 5 shows that if the transmission probability of mutant strains (β_2) increased to $1.8\beta_2$, or the proportion of infecteds with the mutant strain (q) increased to 0.9 (its baseline value is about 0.6), the total death would increase by 181,692 and 117,256 cases, respectively, with an increasing of 0.753 and 0.486% on the mortality rate, respectively. If the vaccination rate Ψ (resp. the infection probability of the vaccinated individuals θ) increased by 80%, the total deaths would decrease by 83,445 (resp. increase by 191,050) and the mortality rate would decrease by 0.346% (resp. increase by 0.792%). If the indirect transmission rate β_w increased by 80%, there would be an increasing of 94,057 on the the total death with an increasing of 0.39% on the mortality rate. Furthermore, we investigated the effect of contact tracing on the containment of the epidemic. If 30, 50 and 70% of infected individuals were contact traced and required to implement social distancing, i.e., the infectious cases (I_w, I_m) decreased by 30, 50, 70%, the total number of deaths would decrease by 79,915, 129,162 and 173,925 and the mortality rate would decrease by 0.331, 0.536

and 0.721%, respectively. The results indicated that the mutant strain and environmental transmission have aggravated the outbreak significantly while the vaccination have alleviated the outbreak greatly. The contact tracing measure also has a significant effect on curbing the epidemic. Countries with large population density and medical resource-constraints like India should strengthen controlling the spread of the mutated strain, accelerate the introduction of booster shots for COVID-19 vaccines, and enhance the clearance of virus from the environment to combat the possible COVID-19 outbreak in future. In the event of a future outbreak of COVID-19 in a similar country, contact tracing should also be implemented due to its imperative role in controlling the epidemic, especially during the early stage of the outbreak.

Among the mathematical modeling studies on the spread of COVID-19 [5, 7, 8, 20, 22–24, 27, 30, 31, 34, 35, 40–45], only a few research focused on the epidemic in India [7, 8, 35, 40]. Khajanchi et al. [7] focused on the effect of contact tracing. They revealed that combining the restrictive social distancing and contact tracing could eliminate the COVID-19 pandemic. Kumar et al. [8] focused on the dynamics of omicron variant virus. They investigated the transmission dynamics of the COVID-19 in India during the omicron variant virus transmission and vaccination drive. Britto et al. [35] concerned the vaccine allocation strategies and demonstrated a relative reduction in deaths if the older population got the priority for the COVID-19 vaccine. Zu et al. [40] concerned the influence of contaminated environments on the transmission of COVID-19 in India. These studies have only analyzed the transmission dynamics of the novel coronavirus when one or two factors are in effect. In fact, in many outbreaks of COVID-19 since 2021, such as the one in India investigated in this work, many a factor played an important role in the spread of the outbreak. That drove us to mimic the combined effects of these factors, including simultaneous transmission of mutant strain and wild strain, environmental transmission, vaccination, shortage of medical resource and contact tracing measures, on controlling the epidemic in India. In this work, we quantitatively assessed the efficiency of each factor in epidemic control in India if the other factors were also effective. We found that both mutant strain and contaminated environments had significant effect on worsening the outbreak even after vaccination was implemented. The vaccine mitigated the outbreak to some extent, although there was mutated strain and environmental transmission. And in cases where multiple factors were in effect at the same time, contact tracing and quarantine still played an imperative role in curbing the epidemic, especially when vaccine effectiveness and vaccine coverage were not high enough.

• *Conclusions*

This paper is the first to mimic the impact of the multiple factors, including mutated strain, environmental pollution, vaccination and resource constraints, on the COVID-19 outbreak in India from 1 March to 1 October, 2021. Our results demonstrated that, in the context of shortage of essential medical resource, the parameters related to the mutant strain ($\beta_2, q, \gamma_2, \alpha_2$) and vaccines ($\theta, \Psi$) are the key parameters and should be prioritized to control the epidemics. The main findings suggest a significant effect of the mutant strain, contaminated environments and vaccination on the spread of the epidemic. Although this study are based on India, the main findings are applicable to other countries with limited medical resources. We found that, to curb the possible future outbreak of COVID-19, inhibiting the prevalence of mutant strain, clearing the virus in the environments as soon as possible, enhancing the vaccination of booster shots and strengthening the contact tracing, especially in the early stage of the outbreak, are required for those countries facing shortage of medical resources.

There are some limitations of our work. The key issue is assessing the impact of mutant strain, environmental transmission and shortage of medical resources. During the outbreak of this wave in India, about 70% of individuals completed the first dose of vaccine, although the percentage completed the full dose was lower, so we modeled the vaccine's protective effect. In fact, it is not ideal to evaluate the efficacy of the vaccine using the epidemic data from India due to the relatively low vaccine coverage in India, especially the low percentage of booster shots completed. It is more reasonable to choose other countries with higher vaccine coverage, such as the United States and Italy, to evaluate the protective effect of the vaccine. In the future work, we will take these countries as examples to study the effect of vaccines in detail. Moreover, it is not very good to use a single model to mimic the transmission dynamics of COVID-19 in the whole country of India since India is a very vast country with many geographical difference. And we have not looked deeply into how the good governance, like improving the effectiveness of administering COVID-19 vaccinations and social distancing, can help mitigate the outbreak [55, 56].

In summary, this study quantitatively assessed the impact of the key factors on the outbreak of the epidemic. The main findings in this work can help those similar countries and policy-making sectors to effectively mitigate against the future possible outbreak.

Acknowledgements

This research was funded by the National Natural Science Foundation of China (grant number: 12271431) and special scientific research project of emergency public health security of education department of Shaanxi province (grant number: 20JG002).Our data are collected from publicly published data, have no privacy implications and can be found in https://voice.baidu.com/act/newpneumonia/newpneumonia/?from=osari_aladin_banner#tab4, https://www.who.int/emergencies/diseases/novel-coronavirus-2019/situation-reports.

Conflict of interest

The authors declare that they have no conflict of interests.

Appendix A

In this appendix, we provided some figures on the sensitivity analysis. We note that during the outbreak of COVID-19 in India from 1 March to 1 October, 2021, many a factor, including the mutant strain, environmental transmission and vaccination, in the context of medical resource-constraints, played a vital role. We have examined the effect of each factor on the spread of the epidemic, and plotted a series of figures at the same time. We inserted some of the figures in the main text and put the others in this appendix. To highlight the effect of these factors on the outbreak of the epidemic, we put the according descriptions and explanations of these figures in the text.

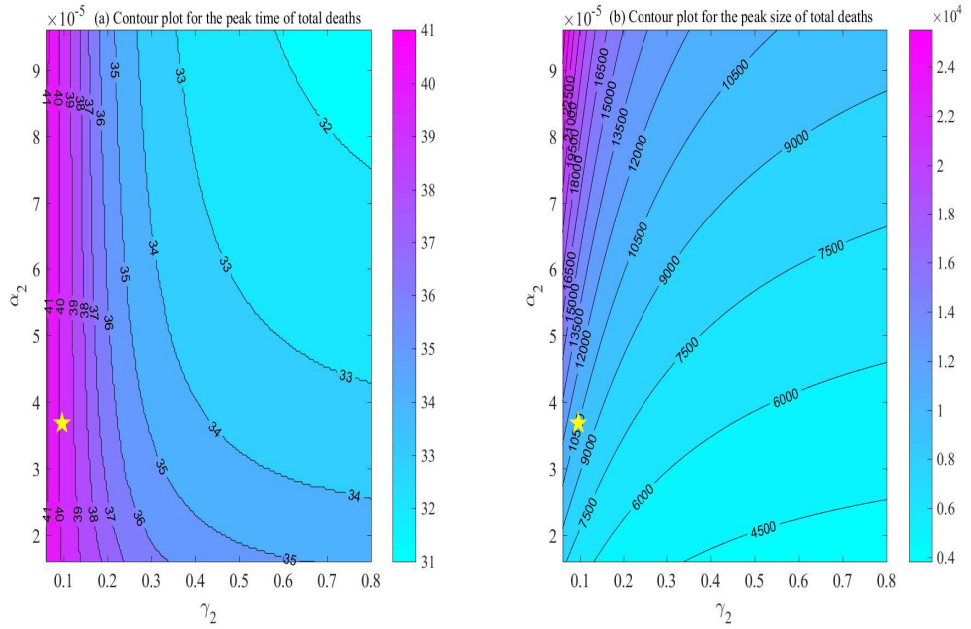

Figure 10. Contour plots of the peak time and peak size of the daily number of total deaths in reality from 1 March to 1 October, 2021 in India to γ_2 and α_2 . The yellow star demonstrates the position of (γ_2, α_2) that we have reported in Table 1.

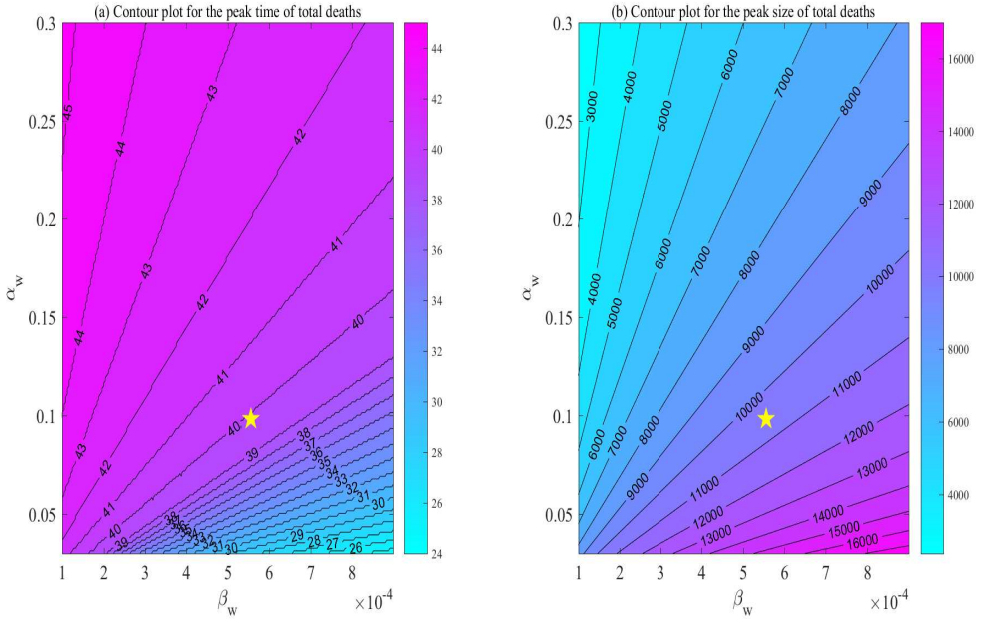

Figure 11. Contour plots of the peak time and peak size of the daily number of total deaths in reality from 1 March to 1 October, 2021 in India to β_w and α_w. The yellow star demonstrates the position of (β_w,α_w) that we have reported in Table 1.

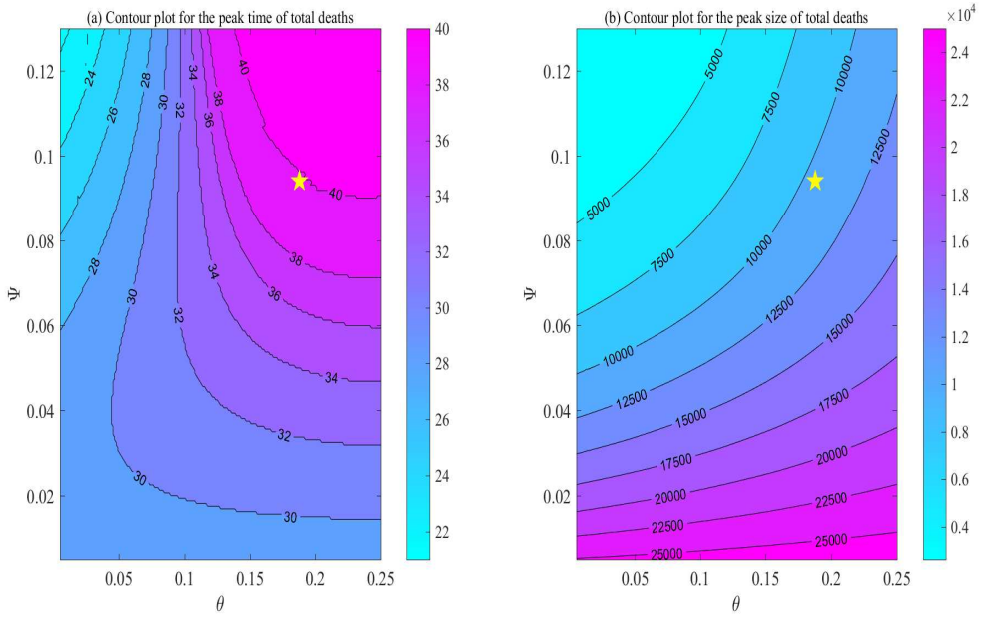

Figure 12. Contour plots of the peak time and peak size of the daily number of total deaths in reality from 1 March to 1 October, 2021 in India to Ψ and θ. The yellow star demonstrates the position of (Ψ, θ) that we have reported in Table 1.

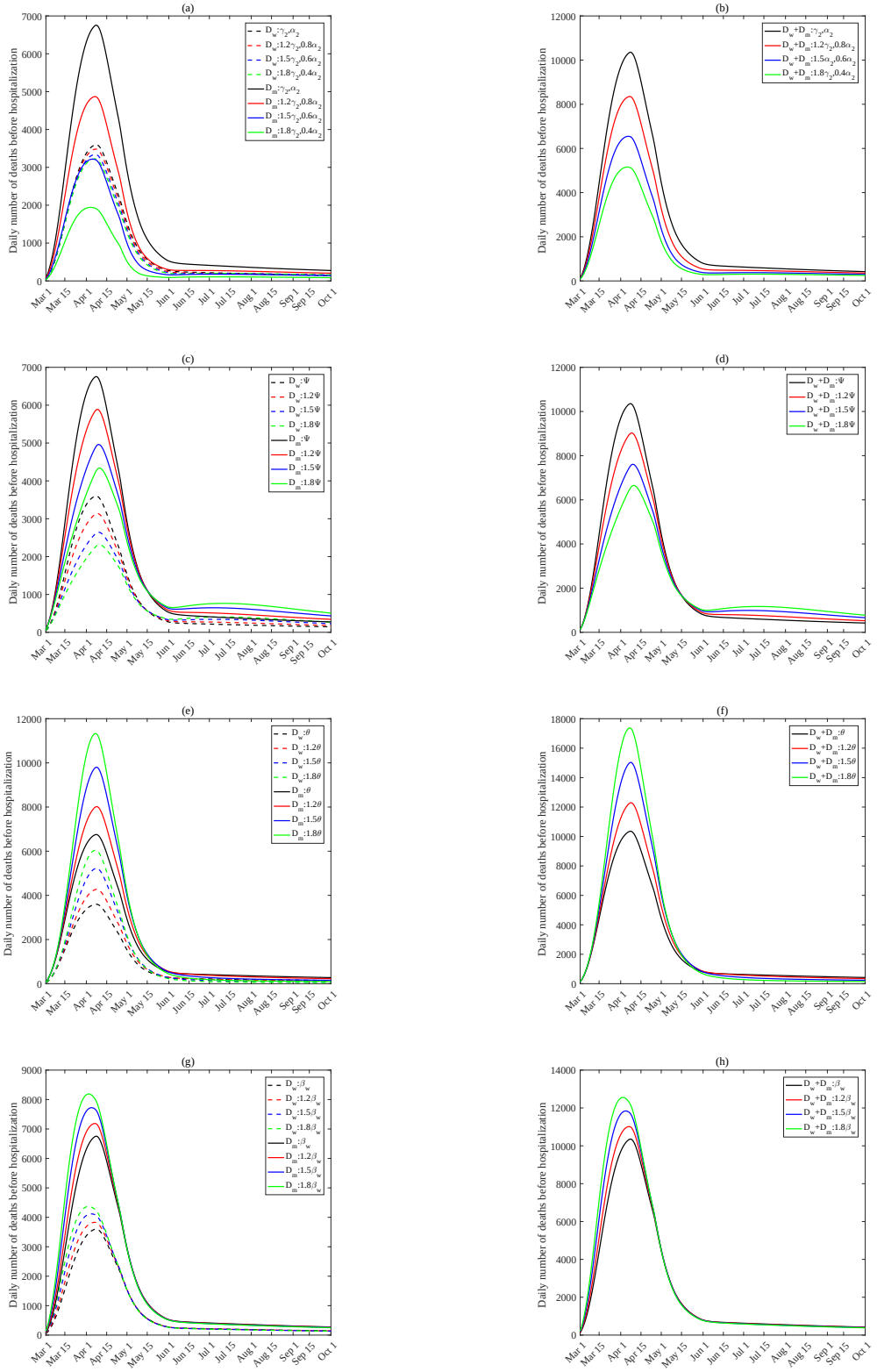

Figure 13. Variation of the daily deaths before hospitalization with different values of $\gamma_2, \alpha_2, \Psi, \theta$ and β_w from 1 March to 1 October, 2021 in India, where D_w and D_m represent daily deaths with the wild strain and the mutant strain, $D_w + D_m$ represents the sum of the daily deaths with the wild and mutant strains.

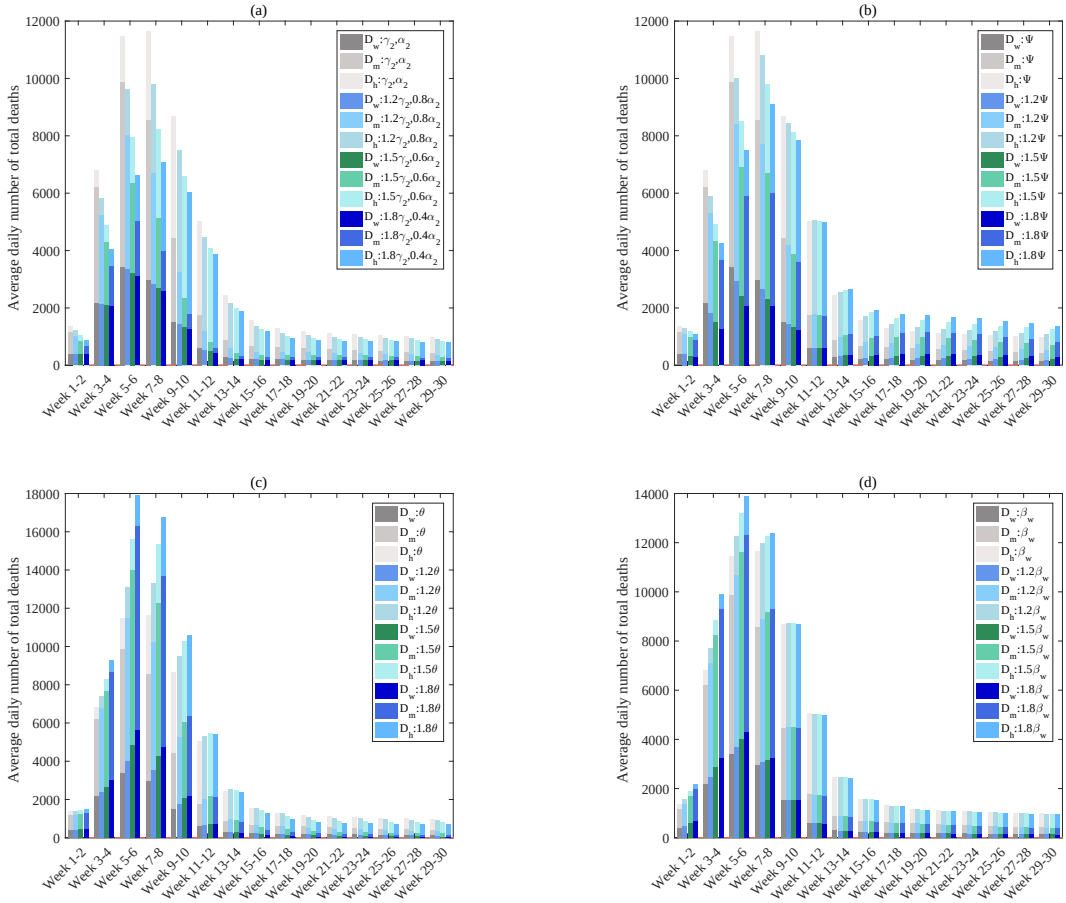

Figure 14. Impact of the mutant strain (γ_2, α_2), vaccination (Ψ, θ) and contaminated environments (β_w) on the total deaths in reality from 1 March to 27 September, 2021 in India. Dark grey, cyan, green and blue represent the average daily deaths with the wild strain before hospitalization (D_w); moderate grey, cyan, green and blue stand for the average daily deaths with the mutant strain before hospitalization (D_m); light grey, cyan, green and blue represent the average daily deaths in the hospital (D_h) every two weeks.

References

1. *World Health Organization*, Coronavirus disease (COVID-19) Weekly Epidemiological Update and Weekly Operational Update, 2022. Available from: https://www.who.int/emergencies/diseases/novel-coronavirus-2019/situation-reports.
2. B. Tang, X. Wang , Q. Li, N. L. Bragazzi , S. Tang, Y. Xiao, et al., Estimation of the transmission risk of the 2019-nCoV and its implication for public health interventions, *J. Clin. Med.*, **462** (2020), 1–13. https://doi.org/10.3390/jcm9020462
3. J. T. Wu, K. Leung, G. M. Leung, Nowcasting and forecasting the potential domestic and international spread of the 2019-nCoV outbreak originating in Wuhan, China: a modelling study, *Lancet*, **395** (2020), 689–697. https://doi.org/10.1016/S0140-6736(20)30260-9
4. M. Al-Yahyai, F. Al-Musalhi, I. Elmojtaba, N. Al-Salti, Mathematical analysis of a COVID-19 model with different types of quarantine and isolation, *Math. Biosci. Eng.*, **20** (2023), 1344–1375. https://doi.org/10.3934/mbe.2023061
5. F. *Özköse*, M. Yavuz, Investigation of interactions between COVID-19 and diabetes with hereditary traits using real data: A case study in Turkey, *Comput. Biol. Med.*, **141** (2022), 105044. https://doi.org/10.1016/j.compbiomed.2021.105044
6. C. Huang, Y. Wang, X. Li, L. Ren, J. Zhao, Y. Hu, et al., Clinical features of patients infected with 2019 novel coronavirus in Wuhan, China, *Lancet*, **395** (2020), 497–506. https://doi.org/10.1016/S0140-6736(20)30183-5
7. K. Sarkar, S. Khajanchi, J. J. Nieto, Modeling and forecasting the COVID-19 pandemic in India, *Chaos Soliton Fract*, **139** (2020), 110049. https://doi.org/10.1016/j.chaos.2020.110049
8. R. P. Kumar, P. K. Santra, G. S. Mahapatra, Global stability and analysing the sensitivity of parameters of a multiple-susceptible population model of SARS-CoV-2 emphasising vaccination drive, *Math. Comput. Simulat.*, **203** (2023), 741–766. https://doi.org/10.1016/j.matcom.2022.07.012
9. Real time big data report on COVID-19, 2022. Available from: https://voice.baidu.com/act/newpneumonia/newpneumonia/?from = osari_aladin_banner#tab4..
10. E. Bontempi, M. Coccia, International trade as critical parameter of COVID-19 spread that outclasses demographic, economic, environmental, and pollution factors, *Environ. Res.*, **201** (2021), 111514. https://doi.org/10.1016/j.envres.2021.111514
11. M. Coccia, Factors determining the diffusion of COVID-19 and suggested strategy to prevent future accelerated viral infectivity similar to COVID, *Sci. Total Environ.*, **729** (2020), 138474. https://doi.org/10.1016/j.scitotenv.2020.138474
12. M. Coccia, COVID-19 pandemic over 2020 (with lockdowns) and 2021 (with vaccinations): similar effects for seasonality and environmental factors, *Environ. Res.*, **208** (2022), 112711. https://doi.org/10.1016/j.envres.2022.112711
13. E. Bontempi, M. Coccia, S. Vergalli, A. Zanoletti, Can commercial trade represent the main indicator of the COVID-19 diffusion due to human-to-human interactions? A comparative analysis between Italy, France, and Spain, *Environ. Res.*, **201** (2021), 111529. https://doi.org/10.1016/j.envres.2021.111529

14. P. Asrani, M. S. Eapen, M. I. Hassan, S. S. Sohal, Implications of the second wave of COVID-19 in India. *Lancet Resp. Med.*, **9** (2021), e93–e94. https://doi.org/10.1016/S2213-2600(21)00312-X

15. O. P. Choudhary, I. Singh, A. J. Rodriguez-Morales, Second wave of COVID-19 in India: dissection of the causes and lessons learnt, *Travel Med. Infect. Dis.*, **43** (2021), 102126. https://doi.org/10.1016/j.tmaid.2021.102126

16. P. Asrani, K. Tiwari, M. S. Eapen, M. I. Hassan, S. S. Sohal, Containment strategies for COVID-19 in India: lessons from the second wave, *Anti-Infect. Ther.*, **20** (2022), 1–7. https://doi.org/10.1080/14787210.2022.2036605

17. S. Ghosh, N. R. Moledina, M. M. Hasan, S. Jain, A. Ghosh, Colossal challenges to healthcare workers combating the second wave of coronavirus disease 2019 (COVID-19) in India, *Infect. Control Hosp. Epidemiol.*, **43** (2021), 1–2. https://doi.org/10.1017/ice.2021.257

18. A. Kumar, K. R. Nayar, S. F. Koya, COVID-19: Challenges and its consequences for rural health care in India, *Public Health Pract.*, **1** (2020), 100009. https://doi.org/10.1016/j.puhip.2020.100009

19. S. P. Mampatta, Rural India vs Covid-19: train curbs a relief but challenges remain, *Bus. Stand.*, **23** (2020).

20. X. Wang, Q. Li, X. Sun, S. He, F, Xia, P. Song, et al., Effects of medical resource capacities and intensities of public mitigation measures on outcomes of COVID-19 outbreaks, *BMC Public Health*, **21** (2021),1–11. https://doi.org/10.1186/s12889-021-10657-4

21. B. Sen-Crowe, M. Sutherland, M. McKenney, A. Elkbuli, A closer look into global hospital beds capacity and resource shortages during the COVID-19 pandemic, *J. Surg. Res.*,**260** (2021), 56–63. https://doi.org/10.1016/j.jss.2020.11.062

22. J. Li, P. Yuan, J. Heffernan, T. Zheng, N. Ogden, B. Sander, et al., Fangcang shelter hospitals during the COVID-19 epidemic,Wuhan, China, *Bull. W. H. O.*, **98** (2020), 830–841D. https://doi.org/10.2471/BLT.20.258152

23. G. Sun, S. Wang, M. Li, L. Li, J. Zhang, W. Zhang, et al., Transmission dynamics of COVID-19 in Wuhan, China: effects of lockdown and medical resources, *Nonlinear Dynam.*, **101** (2020), 1981–1993. https://doi.org/10.1007/s11071-020-05770-9

24. A. Wang, J. Guo, Y. Gong, X. Zhang, Y. Rong, Modeling the effect of Fangcang shelter hospitals on the control of COVID-19 epidemic, *Math. Method Appl. Sci.*, (2022), 1–16. https://doi.org/10.1002/mma.8427

25. Y. Fu, S. Lin, Z. Xu, Research on quantitative analysis of multiple factors affecting COVID-19 spread, *Int. J. Environ. Res. Public Health*, **19** (2022), 3187. https://doi.org/10.3390/ijerph19063187

26. *World Health Organization*, Tracking SARS-CoV-2 variants, 2022. Available from: https://www.who.int/en/activities/tracking-SARS-CoV-2-variants

27. T. Li, Y. Guo, Modeling and optimal control of mutated COVID-19 (Delta strain) with imperfect vaccination, *Chaos Soliton Fract*, **156** (2022), 111825. https://doi.org/10.1016/j.chaos.2022.111825

28. I. Alam, A. Radovanovic, R. Incitti, An interactive SARs-Cov-2 mutation tracker, with a focus on critical variants, *Lancet Infect. Dis.*, **21** (2021), 602. https://doi.org/10.1016/S1473-3099(21)00078-5

29. T. Phan, Genetic diversity and evolution of sars-cov-2, *Infect. Genet. Evol.*, **81** (2020), 104260. https://doi.org/10.1016/j.meegid.2020.104260

30. R. Sonabend, L. K. Whittles, N. Imai, P. N. Perez-Guzman, E. S Knock, T. Rawson, et al., Non-pharmaceutical interventions, vaccination, and the SARS-CoV-2 delta variant in England: a mathematical modelling study, *Lancet*, **398** (2021), 1825–1835. https://doi.org/10.1016/S0140-6736(21)02276-5

31. M. Betti, N. Bragazzi, J. Heffernan, J. Kong, A. Raad, Could a new covid-19 mutant strain undermine vaccination efforts? a mathematical modelling approach for estimating the spread of B.1.1.7 using Ontario, Canada, as a case study, *Vaccines*, **9** (2021), 592. https://doi.org/10.3390/vaccines9060592

32. S. A. Madhi, G. Kwatra, J. E. Myers, W. Jassat, N. Dhar, C. K. Mukendi, et al., Population immunity and COVID-19 severity with Omicron variant in South Africa, *New Engl. J. Med.*, **386** (2022), 1314–1326. https://doi.org/10.1056/NEJMoa2119658

33. M. K. Hossain, M. Hassanzadeganroudsari, V. Apostolopoulos, The emergence of new strains of SARS-CoV-2. What does it mean for COVID-19 vaccines? *Expert Rev. Vaccines*, **20** (2021), 635–638. https://doi.org/10.1080/14760584.2021.1915140

34. O. Khyar, K. Allali, Global dynamics of a multi-strain SEIR epidemic model with general incidence rates: application to COVID-19 pandemic, *Nonlinear Dynam.*, **102** (2021), 489–509. https://doi.org/10.1007/s11071-020-05929-4

35. B. H. Foy, B. Wahl, K. Mehta, A. Shet, G. I Menon, C. Britto, et al., Comparing COVID-19 vaccine allocation strategies in India: A mathematical modelling study, *Int. J. Infect. Dis.*, **103** (2021), 431–438. https://doi.org/10.1101/2020.11.22.20236091

36. *World Health Organization*, Listings of WHO's response to COVID-19, 2020. Available from: https://www.who.int/news/item/29-06-2020-covidtimeline.

37. K. Hattaf, A. A. Mohsen, J. Harraq, N. Achtaic, Modeling the dynamics of COVID-19 with carrier effect and environmental contamination, *Int. J. Model. Simul. Sci. Comput.*, **12** (2021), 2150048. https://doi.org/10.1142/S1793962321500483

38. G. Webb, C. Browne, X. Huo, M. Seydi, O. Seydi, G, Webb, et al., A model of the 2014 Ebola epidemic in West Africa with contact tracing, *PLoS Currents*, **7** (2015). https://doi.org/10.1371/currents.outbreaks.846b2a31ef37018b7d1126a9c8adf22a

39. R. Swain, J. Sahoo, S. P. Biswal, A. Sikary, Management of mass death in COVID-19 pandemic in an Indian perspective, *Disaster Med. Public*, **16** (2022), 1152–1155. https://doi.org/10.1017/dmp.2020.399

40. P. A. Naik, J. Zu, M. B. Ghori, Modeling the effects of the contaminated environments on COVID-19 transmission in India, *Results Phys.*, **29** (2021), 104774. https://doi.org/10.1016/j.rinp.2021.104774

41. S. S. Musa, A. Yusuf, S. Zhao, Z. U. Abdullahi, H. Abu-Odah, F. T. Sa'ad, et al., Transmission dynamics of COVID-19 pandemic with combined effects of relapse, reinfection and environmental contribution: A modeling analysis, *Results Phys.*, **38** (2022), 105653. https://doi.org/10.1016/j.rinp.2022.105653

42. C. Yang, J. Wang, Transmission rates and environmental reservoirs for COVID-19 - a modeling study, *J. Biol. Dynam.*, **15** (2021), 86–108. https://doi.org/10.1080/17513758.2020.1869844

43. M. Mohamadi, A. Babington-Ashaye, A. Lefort, A. Flahault, Modeling the effects of the contaminated environments on COVID-19 transmission in India, *Results Phys.*, **29** (2021), 104774. https://doi.org/10.1016/j.rinp.2021.104774

44. P. A. Naik, M. Yavuz, S. Qureshi, J. Zu, S. Townley, Modeling and analysis of COVID-19 epidemics with treatment in fractional derivatives using real data from Pakistan. *Eur. Phys. J. Plus.*, **135** (2020), 1–42. https://doi.org/10.1140/epjp/s13360-020-00819-5

45. P. A. Naik, K. M. Owolabi, J. Zu, M. Naik, Modeling the transmission dynamics of COVID-19 pandemic in Caputo type fractional derivative. *J. Multiscale Model.*, **12** (2021), 2150006. https://doi.org/10.1142/S1756973721500062

46. *The Guardian*, Death and despair at the doors of stricken Delhi hospital, 2021. Available from: https://guardian.ng/news/death-and-despair-at-the-doors-of-stricken-delhi-hospital

47. *Global News*, India's COVID-19 needs are large and diverse. Doctors, aides welcome global help, 2021. Available from: https://globalnews.ca/news/7819412/india-covid-crisis-doctors-red-cross

48. V. Strejc, Least squares parameter estimation, *Automatica*, **16** (1980), 535–550. https://doi.org/10.1016/S1474-6670(17)53975-0

49. M. A. Khan, A. Atangana, Modeling the dynamics of novel coronavirus (2019-nCov) with fractional derivative, *Alex Eng. J.*, **59** (2020), 2379–2389. https://doi.org/10.1016/j.aej.2020.02.033

50. P. Driessche, J. Watmough, Reproduction numbers and sub-threshold endemic equilibria for compartmental models of disease transmission, *Math. Biosci.*, **180** (2002), 29–48. https://doi.org/10.1016/S0025-5564(02)00108-6

51. S. Marino, I. B. Hogue, C. J. Ray, D. E Krischner, A methodology for performing global uncertainty and sensitivity analysis in systems biology, *J. Theor. Biol.*, **254** (2008), 178–196. https://doi.org/10.1016/j.jtbi.2008.04.011

52. *Daily News*, India crosses 300,000 COVID deaths, 2021. Available from: https://www.dailynews.lk/2021/05/24/world/250039/india-crosses-300000-covid-deaths.

53. *Global News*, India has 414K COVID-19 deaths to date. The actual toll could be 10 times higher, 2021. Available from: https://globalnews.ca/news/8042640/india-covid-19-deaths-toll-10-times-higher/.

54. C. Z. Guilmoto, An alternative estimation of the death toll of the Covid-19 pandemic in India, *PloS One*, **17** (2022), e0263187. https://doi.org/10.1371/journal.pone.0263187

55. M. Coccia, Optimal levels of vaccination to reduce COVID-19 infected individuals and deaths: A global analysis. *Environ. Res.*, **204** (2022), 112314. https://doi.org/10.1016/j.envres.2021.112314

56. I. Benati, M. Coccia, Global analysis of timely COVID-19 vaccinations: improving governance to reinforce response policies for pandemic crises. *Int. J. Health Gov.*, **27** (2022), 240–153. https://doi.org/10.1108/IJHG-07-2021-0072

AIMS Press